University of South-Eastern Norway

www.usn.no

FMH606 Master's Thesis 2021
Electrical Power Engineering

Evaluation of battery storage in combination with hydro-power systems

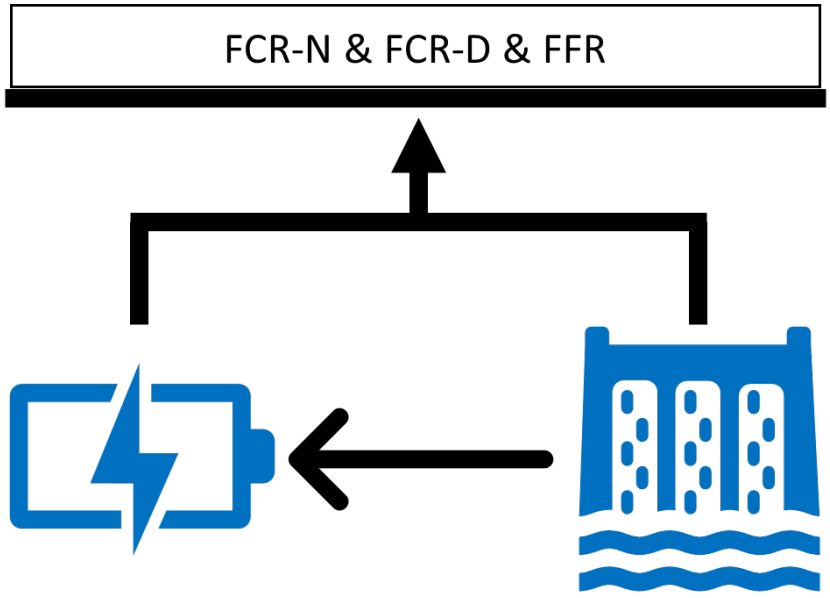

Lars Jonatan Hellborg

Faculty of Technology, Natural Sciences and Maritime Sciences
Campus Porsgrunn

University of South-Eastern Norway

www.usn.no

Course: FMH606 Master's Thesis 2021
Title: *Evaluation of battery storage in combination with hydro-power systems*
Pages: *115*
Keywords: *Hydro-power, Battery, Energy storage, Ancillary services, Power reserves, Frequency regulation*

Student: *Lars Jonatan Hellborg*
Supervisor: *Dietmar Winkler*
External partner: *Norconsult, Uniper*

Summary:
As the power grid moves away from larger rotating masses, thereby decreasing the inertia and making the grid more sensitive to production changes, it becomes more and more important that new and improved power reserves are implemented.
Battery storage systems are a great tool for providing the ancillary services that are required in order to ensure the stability of the grid- but, they do suffer from a flaw in that they are limited. This flaw can, as is shown in this thesis, be mitigated by installing the battery energy storage in connection with hydro-power units and allowing them to increase production to offset the battery output if the frequency deviation persists. This Thesis contains a technical study which details the various parts of this type of hybrid system as well as discussing the various benefits and future scenarios. Furthermore, it contains an evaluation of the work done by Uniper, which also serve as the foundation of this Thesis.

The evaluation of installed units at Lövön clearly shows that the technical requirements, as stipulated by SVK in conjunction with the rest of the Nordic TSOs, are fulfilled. Furthermore, while the developed models are not an exact replica of the installed units, they do exhibit the same behaviour and provide realistic, verified results as well as providing a base for future developments.

The models and simulations show that this type of hybrid system can greatly reduce the wear and tear on the turbines, while still being able to provide the required functions.

Preface

This thesis is the conclusion of a two-year Master's program in the field of Electrical Power Engineering at the University of South-Eastern Norway. The work done throughout this Thesis work was made in conjunction with the external partners Norconsult and Uniper based on a previous project completed by the latter in which battery storage was installed in connection with hydro-power units.

Overall, the project went well despite the challenges that came from the pandemic that was going on at the time of writing. However, due to the lack of time some features of the developed model were not included and present an opportunity for future development.

I would like to extend my gratitude to the people who have helped me throughout the writing, such as Robert and Hans-Åke at Norconsult. They were both invaluable throughout the Thesis work and the report would not be what it is today without them. Furthermore, I would like to thank Assar and Erik at Uniper, whom both provided invaluable information and assistance. A special thanks goes out to my supervisor at the university, Dietmar Winkler, whom provided comments and feedback throughout the writing process. Furthermore, i would like to thank Tyler C. Janssen and Samuel Hodge for their help in proofreading and making sure the grammatical rules are adhered to.

Last but not least, I would like to extend my greatest thanks to Frida Grebner Nord with whom I have shared many a conversation with when my stress and frustration were immense. Thank you!

Porsgrunn, 17th May 2021

Lars Jonatan Hellborg

Contents

List of Figures

List of Tables

Nomenclature

Acronyms

AC : Alternating Current

aFRR : Automatic Frequency Restoration Reserve

BESS : Battery energy storage system

DC : Direct Current

FCR-D : Frequency Containment Reserve - Disturbance

FCR-N : Frequency Containment Reserve - Normal

FESS : Flywheel energy storage system

FFR : Fast Frequency Reserve

HBHS : Hybrid Battery/Hydro system

HVDC : High-Voltage Direct Current

LER : Limited Energy Reservoir

mFRR : Manual Frequency Restoration Reserve

RoCoF : Rate of Change of Frequency

SOC : State of charge

SVK : Svenska Kraftnät

Concepts

Dimensioning incident : Largest expected disturbance that can happen, which the system needs to manage. Currently the loss of Oskarshamn 3 (1450 MW)

Market liquidity : Market liquidity is the ability of a market whereby individuals and firms can quickly buy or sell assets without causing large changes in the assets price.

N-1 Criterion : This criteria means that the power system should be able to deal with the loss of a main component, yet still manage to uphold operational security

Symbols

Δf : Change in system frequency [Hz]

ΔP_{cons} : Change in system consumption [W]

ω_i : Machine angular speed [rad/s]

ρ : Material density [kg/m^3]

σ : Material tensile strength [Pa]

D : System damping [MW/Hz]

E : Rotor kinetic energy [J]

h_{res} : Reservoir level [m]

h_{tail} : Tail-water level [m]

H_g : Gross head [m]

H_n : Net head [m]

J_i : Machine inertia [kgm^2]

J_{sys} : Total system inertia [J]

K : Rotor geometric shape factor [−]

m : Rotor mass [kg]

P_{cons} : Total system consumption [W]

$P_{electrical}$: Braking electrical power [W]

P_{mech} : Driving mechanical power [W]

P_{prod} : Total system production [W]

1 Introduction

One of the fundamental rules of the modern power grid is that the consumption is equally balanced with the production. Should this not be the case, the frequency of the grid will start to deviate from the nominal value which will cause problems and eventually blackouts. To make sure that the frequency of the grid is kept stable at its nominal value, the Nordic power grid uses three different types of production reserves: Primary, Secondary and Tertiary reserves.
The main difference between these three types is the time-scale at which they operate with Primary being the fastest to act and Tertiary being the slowest.

While hydro-power systems are commonly used for frequency regulation in Sweden, they are not designed for the fast regulation needed to allow them to be a part of the primary production reserve nor the new faster reserves being implemented. As the technical requirements from the Nordic TSOs become stricter, the currently participating hydro-power units need to be optimized or they risk being stripped of their pre-qualification. One possible solution to this problem is the installation of battery storage units in conjunction with these hydro-power units.

Due to this, Uniper, which is a Germany based energy company with a range of assets in Sweden, have been working on two different projects where battery storage units were installed in combination with hydro-power systems at two locations in order to enable them to sell frequency regulation from machines that are not designed for this type of fast regulation.

1.1 Objectives and scope

The purpose of this thesis is three-fold:

- Produce an in-depth technical study into how battery storage can be used in conjunction with hydro-power to provide frequency containment reserve from units not designed for this purpose.
- Give an outside evaluation of the previous project headed by Uniper where battery storage was installed at two hydro-power plants.

- Highlighting the potential gains with this technology through simulations and models.

The technical study aims to not only detail the various components needed to connect battery storage to the hydro-power plants but also determine other possible gains that can be found, such as the possibility of using the battery storage for things other than frequency regulation and using them in conjunction with solar power. The study should also evaluate the technological progress that can be expected in the future, as well as assess the project from a sustainability perspective.

Furthermore, by developing a model that represents the hybrid system and comparing this to models of more traditional systems, any potential gains (such as reduced maintenance) will be highlighted. This model should be verified against previous research as well as against measurements taken from the installed units at Lövön and Edsele.

1.2 Methodology

The work done throughout this Master's Thesis was split into three main parts; literature study, modelling and evaluation. The first part, the literature study, aimed to provide a deeper understanding of the field as well as providing the basis on which the technical study is based. This part also aimed to collect the information required for the modeling, simulations and provide the knowledge to facilitate these parts. The literature study was accomplished by mapping out the previous research that had been done on the various parts of the BESS, and determining if any work has been done on the hybrid system.

Based on data and information collected in the previous part, models were developed in MATLAB/Simulink. These models were then verified against the previous research in order to determine their viability. Furthermore, the information received from the external partners helped to create a model which is as close to the installed units as possible.

Lastly, for the evaluation of the previous project interviews were held with key project members which were then collated and summarized. This, in addition to the measurements provided from Lövön and Edsele, was then used for the actual project evaluation with the goal of collating the various findings and lessons that should be used for future projects similar to this.

1.3 Structure

The report has the following structure:

Chapter 2
This chapter contains info about the relevant underlying theory of the power grid, as well as explanations regarding the current laws and rules for reserves in the Swedish power grid.

Chapter 3
This chapter contains the technical descriptions for the components used in the implemented systems, as well as describing the components from a sustainability and versatility perspective.

Chapter 4
Contains the theory and methodology behind the developed models as well as explanations regarding the key process indicators used to determine the suitability of the models

Chapter 5
Contains the results from the simulations performed on both the traditional units as well as the hybrid system.

Chapter 6
Presents the evaluation of the implemented units at Lövön and Edsele, with focus being on how well the system fulfills the function as well as discussing what lessons to bring to the next project.

Chapter 7
This chapter contains the discussion regarding the results of this project, both regarding the technical study but also the project evaluation and simulations.

Chapter 8
This final chapter describes the conclusions which can be drawn from the report based on the presented data and information.

2 Background/Theory

2.1 Electrical grid

Sweden has one of the worlds oldest electrical grids, dating back to 1952 when the worlds first 400 kV line was installed between Storfinnforsen and Midskog [1]. The current electrical grid, much like the grids in Norway and Finland [2][3], is divided into three different grid levels: Transmission, Regional and Distribution. Historically speaking, the main bulk of Sweden's production has been situated in the northern part where most of the large hydro-power plants are found while most of the consumption is found in the southern parts.

Transmission grid

The transmission grid has the highest voltages throughout the electrical system, between 220 - 400 kV, and transmits the power from the production units to the various regional grids. This grid, which also contains High-Voltage Direct Current (HVDC) connections and various transformer/switching stations, spans the entire country, as seen in Figure 2.1. The transmission grid also has connections to the neighbouring countries. These connections to countries such as Finland, Norway, Denmark and Lithuania (among others) enable the export and import of energy. This grid is owned by the government and operated by the Transmission System Operator, or TSO, which in Sweden's case is Svenska Kraftnät (SVK). The TSO has the overall responsibility over the entire electrical systems.

Regional grid

This grid level, which usually uses a voltage between 20 and 130 kV [4], connects the transmission grid to the larger consumers. These consumers consists of larger industries but also the distribution grids. The Swedish regional grids are mostly owned by three companies; Vattenfall, E.ON and Ellevio, whom supply a majority of the electricity users in Sweden [4].

Distribution grid

These grids make up the majority of the total lengths of lines found in the the total system and connect the regional grids to the consumers such as households and smaller industries. From the voltage level in the regional grid, the voltage is transformed down to a voltage level of 400 V.

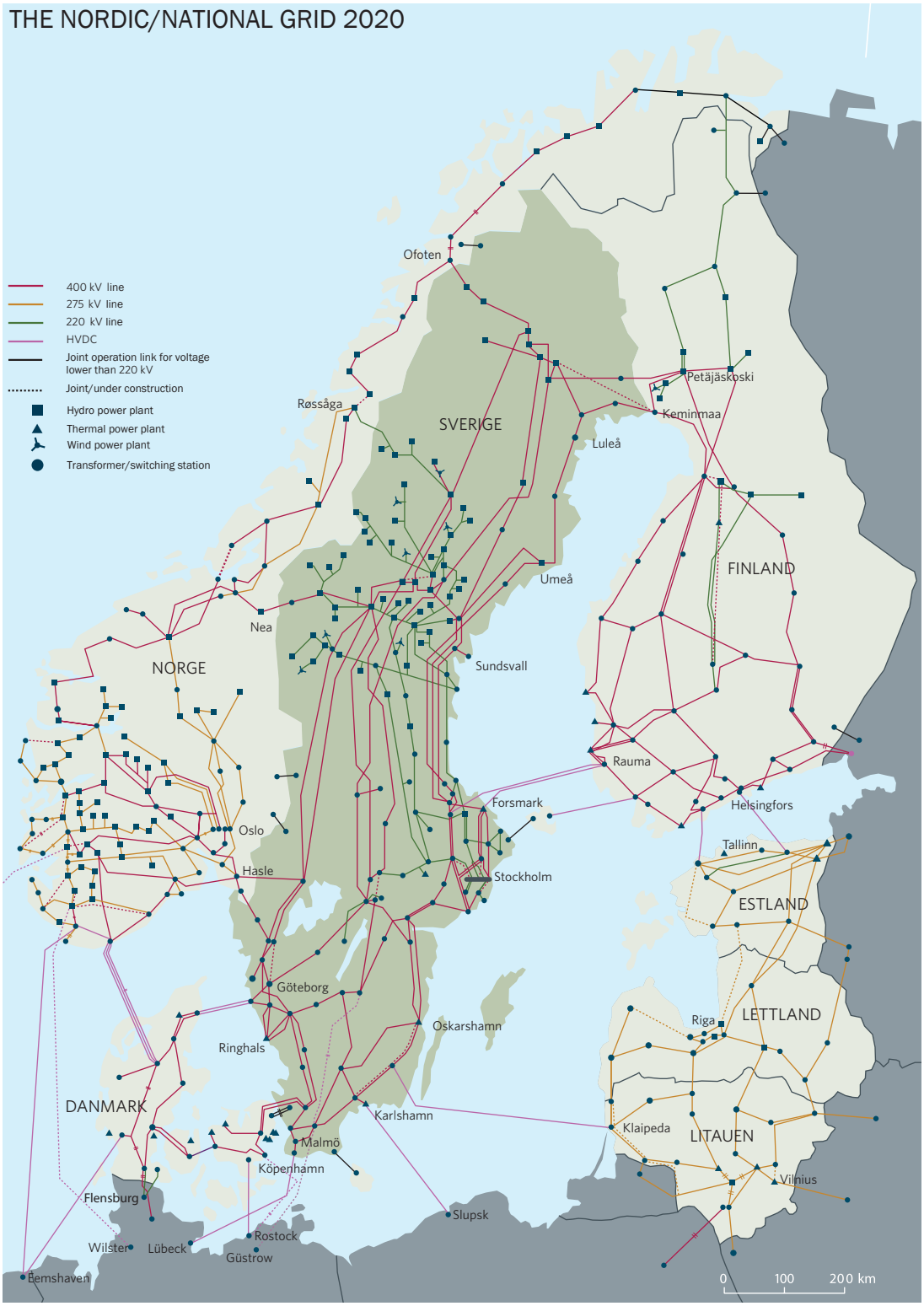

Figure 2.1: Map of the Nordic transmission grid [5]

Figure 2.2: Map over electricity price areas in the Nordic grid [7]

Ever since 2011, Sweden's electricity grid has been divided into four separate areas, each with their own electricity price, as seen in Figure 2.2. Area SE3 and SE4, which encapsulate the southern part of Sweden, are where most of the consumption is found while area SE1 and SE2 generally have had a surplus of electricity due to large production but low consumption. This difference in consumption and production in the various areas means that the price for electricity can vary between the areas, where SE1 and SE2 tend to be cheaper while the opposite is true for SE3 and SE4. Part of the reason behind this division was to ensure Sweden would follow the rules stipulated by EU, but also to promote electricity heavy industries to establish themselves in the northern parts, where electricity is cheaper [6].

2.2 Balancing and ancillary services

2.2.1 Inertia

Inertia is a fundamental concept throughout physics, described by Newton in his Philisophiae Naturalis Principia Mathematica [8] as:

> The vis insita, or innate force of matter, is a power of resisting by which everybody, as much as in it lies, endeavours to preserve its present state, whether it be of rest or of moving uniformly forward in a straight line.
>
> (Newton)

For the power grid, inertia is an important parameter because it directly affects the rate of change of frequency (or RoCoF) making the grid more resistant to changes and therefore more resistant against disturbances. This is illustrated in Figure 2.3 which highlights the different frequency response for two systems, one with high inertia and one with low, after the loss of a generator. When the generator disconnects, the system with low inertia will not only experience a faster frequency deviation but as a consequence of this also a lower minimum frequency. This means that in order to protect the system against involuntary load shedding, which can be a consequence of having a too low frequency, the reserves must be quicker in their response for systems with low inertia.

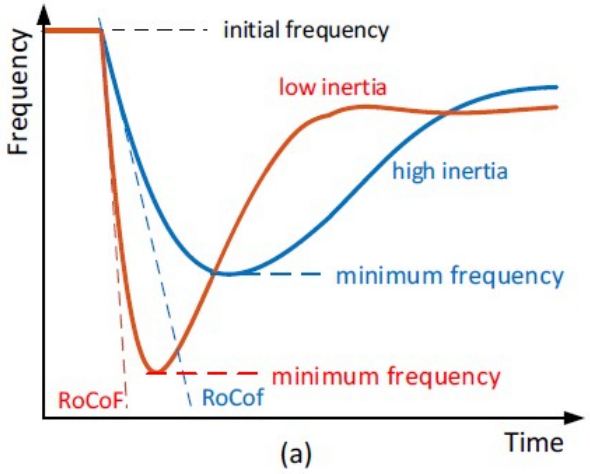

Figure 2.3: Frequency response for systems with high and low inertia [9].

Most of the inertia found in the power grid comes from the large rotating masses, such as synchronous generators from nuclear- and hydro-power, which means that one of the unintended consequences from the shift to renewable energy is the decrease of the grid inertia. This in combination with an increase of intermittent energy types, such as the aforementioned wind and solar, has lead to a decrease in frequency stability and made it necessary with faster acting reserves, such as FFR (described in Section 2.2.5).

2.2.2 Primary reserve

Also known as the frequency containment reserve, or FCR, this reserve is one of the fastest acting and can be further split into disturbance and normal which works in slightly different time-scales. FCR-D, i.e., the disturbance reserve, operates within a few seconds while the normal reserve, i.e., FCR-N, within a few minutes. The main objective of this reserve is to contain the frequency and not let the deviation continue. This reserve will not aim to restore the frequency but rather stop the frequency from deviating further.

Both FCR-D and FCR-N are automatic reserves that require no human input but they differ in operational principles. FCR-N is used to contain the frequency within the nominal frequency range of 49.9 to 50.1 Hz (for the European grid), and activates automatically when the frequency deviates from 50 Hz while still within this range. However, during larger grid disturbances, such as loss of major production units, when the frequency sinks below 49.9 Hz, FCR-D will activate instead [10].

Historically, in Sweden, FCR-N has been provided by hydro-power units due to the ease of control this energy type provides, and of the automatic reserves hydro-power provides close to 100 % [11].

The technical requirements that units must fulfill in order to be qualified to deliver these reserves is summarized in Table 2.1, which also highlights the difference between the requirements for FCR-N and FCR-D. The units aiming to provide FCR-D must, as can be seen in the table, activate faster than FCR-N.

2.2.2.1 FCR-D down

As a further compliment to the primary reserve, mainly FCR-D, the Nordic TSOs are jointly implementing a new ancillary service called ”FCR-D Down” to provide further stabilization possibilities to the power grid. The purpose behind the service is to provide better ways of handling frequencies higher than normal that occur during disturbances.

The units providing this service will therefore lower the production or increase the consumption, which happens linearly between 50.1 and 50.5 Hz. The technical requirements for FCR-D down, as stipulated by the Swedish TSO, is summarized in Table 2.2.

2.2.3 Secondary reserve

The secondary reserve, also known as the Frequency Restoration Reserve or FRR, is the second reserve to act and will do so after the primary reserve. Where the primary reserve contains the frequency, the secondary reserve will restore it to the nominal value.

Table 2.1: Technical demands for FCR-N and FCR-D [12]

	FCR-Normal	FCR-Disturbance
Minimum bid-size	0.1 MW	0.1 MW
Activation criteria	Automatically for frequency deviations within 49.9 - 50.1 Hz	Automatically for frequency deviations under 49.9 Hz
Activation time	63 % within 60 s and 100 % within 3 min.	50 % within 5 s and 100 % within 30 s.
Endurance	At least one hour.	At least one hour.
General demands		
	• Pre-qualified • Real-time measurements • Electronic communication	• Pre-qualified • Real-time measurements • Electronic communication
Miscellaneous	Capable of up- and downward regulation	

There are two version of this reserve, one being automatic (aFRR) and one being manual (mFRR), both of which are used in today's power grid.

aFRR will activate automatically based on a centralized control signal as the frequency starts to deviate from the nominal value. As stipulated in the agreement with SVK the aFRR needs to be fully activated within two minutes [10]. For the manual reserve, i.e., mFRR, the activation time is required to be within 15 minutes and is meant to be a compliment to the automatic type.

Table 2.3 shows the summarized technical requirements for the secondary reserve, or aFRR.

Table 2.2: Technical demands for FCR-D Down [12]

	FCR-Disturbance
Minimum bid-size	0.1 MW
Activation criteria	Automatically for frequency deviations within 50.1 - 50.5 Hz
Activation time	50 % within 5 s and 100 % within 30 s.
Endurance	At least 20 minutes counted from 30 seconds after activation.
General demands	• Pre-qualified • Real-time measurements • Electronic communication

Table 2.3: Technical demands for aFRR [12]

	aFRR
Minimum bid-size	5 MW
Activation criteria	Automatically via centralized control signal when frequency deviates from 50 Hz
Activation time	100 % within 120 s.
Endurance	At least one hour.
General demands	• Pre-qualified • Real-time measurements • Electronic communication

2.2.4 Tertiary reserve

The tertiary reserve is the slowest of the reserves and is manually activated with the goal of replacing the secondary reserve in order to once again make the secondary reserve available for any potential disturbance. The tertiary reserve usually operates in a time-span of between 15 to 60 minutes and for the Nordic grid, the manual frequency restoration reserve, mFRR, fulfills this role.

Figure 2.4 shows how the reserves would operate after a power system imbalance in order to stop the deviation and restore the frequency to the nominal value and Table 2.4 shows the summarized requirements for this type of reserve.

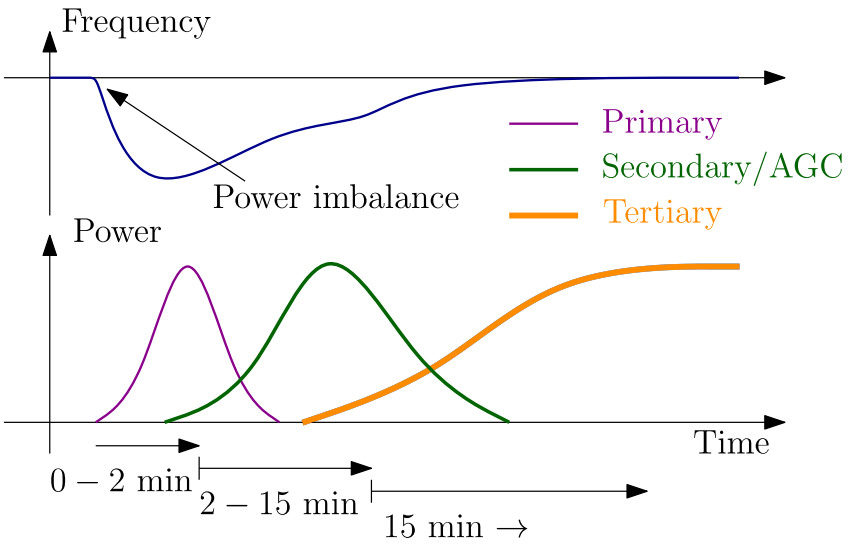

Figure 2.4: Activation of reserves as a consequence of a power imbalance [13].

Table 2.4: Technical demands for mFRR [12]

	mFRR
Minimum bid-size	10 MW (5 in SE4)
Activation criteria	Manually by request from SVK.
Activation time	Within 15 min (Longer time can be allowed)
General demands	Same as for secondary.

2.2.5 Fast frequency reserve

This new reserve, Fast Frequency Reserve or FFR, which is currently undergoing testing and pilot trials to accommodate the implementation into the Nordic power grid is meant to be a compliment to FCR-D, not a replacement.

There are four main aspects to the technical requirements regarding FFR; Activation, Deactivation, Recovery and Repeatability.

Activation

This aspect deals with requirements such as: Minimum support duration, activation level and maximum full activation time. While the minimum support duration will depend on whether the reserve is specified as short or long, the requirements regarding activation level and maximum full activation time will be the same regardless. There are three different allowed combinations of activation level and maximum full activation time, which the provider is free to choose between as long as the choice is specified beforehand, which are described in Table 2.5.

Table 2.5: Activation levels for FFR [14]

Alternative	Activation level [Hz]	Maximum full activation time [s]
A	49.7	1.30
B	49.6	1.00
C	49.5	0.70

Deactivation

The requirements regarding deactivation of FFR state that the unit must be ready for a new cycle within 15 minutes of the activation and that long support duration FFR has no limit in deactivation rate. However, short duration FFR is limited to a maximum of 20 % of the pre-qualified capacity per second [14] as well as no single step larger than 20 %.

Recovery

The FFR unit must be able to be ready for a new cycle in a maximum of 15 minutes. The unit can be dimensioned to either provide several cycles before recovery or initiating recovery after each cycle. While no requirements exists for the shape of the recovery, which can be in the form of a step, there are requirements regarding the magnitude which must not exceed 25 % of the pre-qualified capacity.

Additionally the recovery should not start before a time equal to the sum of the activation time, support duration, deactivation time and ten seconds has passed.

Repeatability

As mentioned previously, the FFR unit must be ready for a new cycle in a minimum of 15 minutes. This requirement, however, is not valid should the frequency still be below 49.8 Hz and the FFR is still active in the electrical grid.

Each of these requirement are, in detail, described in the first version (1.0) of the provisions written by the Inertia2020 group working under ENTSO-E [14] which also contain requirements regarding real-time telemetry and data logging not described here.

2.2.6 Reserve market

Alongside the regular marketplace, where electricity is sold and bought by various actors, is the reserve market. This marketplace has the Nordic grid TSOs buy reserve power in order to handle any eventual disturbances or discrepancies in the grid in order to ensure frequency stability.

A call for bids is made by SVK, who then select the winning bids to provide reserve power during specified time periods. Bids are submitted by various entities - typically large production units - who undertake to provide the power at the agreed upon price should the need for it arise. Each of the previously mentioned reserve types have their own bidding periods where, for example, bids regarding FCR (both FCR-N and FCR-D) are accepted on two occasions, one day and two days ahead of the delivery date. aFRR, on the other hand, is accepted on each Thursday for the coming Saturday-Friday period and mFRR is accepted as needed, i.e., no set dates.

In order for an actor to become a reserve provider, certain requirements need to be met. These requirements will differ between the various reserves but in general they contain requirements pertaining to the market side, such as how bids are to be structured and delivered, as well as more technical demands, such as allowed measurement uncertainties. The exact requirements stipulated can be found in the Balance Responsibility Agreement [10]. The reader should be aware this document is only available in Swedish, and described in the corresponding sections below.

One requirement that applies regardless of the reserve type is the requirement that states that in order for an actor to deliver reserves, they need to preside over units and/or groups of units that are pre-qualified to deliver the specified reserve. For units or groups of units which aim to deliver FCR or FRR this qualification needs to be renewed:

- Every fifth year.
- If the technical demands, equipment requirements or equipment has changed.
- If the equipment related to activation of FCR has been modernized.

This pre-qualification aims to test the ability of the proposed units and to show that the requirements stipulated in the agreement, both technical and market related, are fulfilled by the units [15].

2.2.7 Limited energy reservoirs

The requirements described in Section 2.2.2, 2.2.3 and 2.2.4 pertain to conventional balance reserves, i.e., power generation units such as hydro-power plants and condensation power, but as the power grid is constantly changing and evolving new options need to be made available. These options include, among other things such as the previously mentioned FFR, the ability to provide reserves from limited energy reservoirs (LER). As batteries, and other energy storage, become cheaper it is vital that these are integrated on the ancillary market found throughout Europe. The defined guidelines as to how this implementation is to be done can be found in the System Operations Guideline (SOGL), more specifically article 156 which relates to the provision of FCR [15].

Based on these guidelines SVK has defined new requirements, as well as altered already existing ones, for units who wish to provide reserves from LERs. These added requirements, as described in Table 2.6, include demands on endurance and availability of the units as well as requirements regarding recovery time. While no specific requirements regarding recovery of FCR-N exists, the recovery must not impact the delivery of the reserve. The recovery time, as well as the activation time, needs to be taken into account when the actor makes a bid. For example, in the case of a FCR-N unit with the recovery time of two hours, bids can only be sent in for every third hour.

Table 2.6: Added technical requirements regarding LER [16]

	FCR-Normal	FCR-Disturbance
Endurance	Full activation and continuous availability for at least one hour.	Full activation for at least 20 minutes.
Recovery	No specific time requirements, but must be taken into account for bids, and must not impact delivery of reserve.	Recovery as soon as possible, within two hours.

SVK are currently undertaking a pilot trial where LERs are used for FCR-D and bidding happens continuously throughout the day. The idea behind the trial is to increase the market liquidity as well as learn more about how these new resources work together with the power grid. During this trial providers announce their interest to participate during

pre-qualification of units and the LER-resources are thus allowed to participate on the FCR-D market if the following requirements are fulfilled:

- Description of recovery strategy is approved by SVK.
- Actor saves data about remaining energy, which can be transmitted on demand.
- Other technical demands are fulfilled and approved during pre-qualification.

The pilot trial aims to step-wise increase the total allowed volume from 20 MW up to 60 MW by the end of 2021, but the volume and time span can change during the trial period. The hope is that after the trial is completed, a larger share of LERs can be allowed to participate on the market permanently, under the same terms as during the trial.

2.2.8 Future of ancillary services in the Nordic grid

The power grid is in constant change with new production types such as photo-voltaic cells and wind-power being introduced at a greater rate than ever before [17]. In order to ensure a safe and reliable operation of the grid, the ancillary services must be adapted to the increased amount of intermittent production as well as the lower inertia, which is done by tightening the technical demands on existing services as well as introducing new ones.

Among the most recent services to be added is the Fast Frequency Reserve, which is designed to deal with situations with lower inertia, and FCR-D up which is meant to stabilize the grid during disturbances.

One of the suggested changes to the pricing system for FCR was the move from a cost-based pricing model where actors get paid based on their respective bids (so called pay-as-bid) into a system with free and marginal-based pricing (so called pay-as-cleared). A study performed by the Austrian Institute of Technology came to the conclusion that by changing from cost-based to free bidding the bids would divert from the true cost by almost 80 % of the time for pay-as-bid and more than 60 % for marginal-based pricing.

A follow-up project to this was proposed, and is slated for delivery in the Spring of 2021, that should contain a description as to how this change should be implemented as well as answers to questions regarding thing such as asymmetrical bids. These changes, if implemented, would mean that the ancillary market would be prone to more competition between actors in the FCR-N market.

In order to ensure a secure operation within the Nordic system, the TSOs involved; Fingrid, Statnett, Svenska Kraftnät and Energinet, initiated a joint venture. The goal of this collaboration, known as the Nordic Balancing Model (NBM), is to harmonize the various technical demands regarding ancillary services (mainly FCR-N) and to facilitate the upcoming energy transition.

While it is hard to say whether or not the technical demands are becoming more or less strict, it is clear that they are in constant change. A good example of this is the activation time for aFRR, with SVK currently stipulating a maximum activation time of 120 seconds, but with a new suggestion this time would be 5 minutes. Furthermore, the Nordic TSOs have decided on a few changes to the technical demands regarding FCR-N and FCR-D that would add a bit more leniency. The suggestion involved a lower number of sinusoidal tests and softening FCR-D demands by allowing control parameters which during a short time period only needs to fulfill a limited stability requirement. Beyond this, the changes also include a clearer specification of the technical demands regarding deactivation, usage of LERs and regarding resources with central control and aggregated resources [18].

3 Technical study

3.1 Overarching system description

There are several potential ways to achieve a strong synergy between batteries and hydro-power. Two potential combinations are the hydro-recharge HBHS and the split frequency HBHS, which both produced significant reductions of the wear and tear on the hydro-power units in simulations [19].

Because the battery energy storage systems have the capability to react to frequency deviations faster than most (if not all) hydro-power plants the most common implementation of the hybrid system is to use the battery to provide the reserve power and recharge the battery using the hydro-power plant. This is the implementation used by Fortum in their project at Forshuvud near Trollhättan in Sweden and Uniper at Edsele and Lövön [20].

The general idea of the implemented hybrid system (hydro-recharge in the case of Lövön and Edsele) is that the installed battery will only need to supply enough power to mitigate the frequency deviation. Should the deviation persist for a longer period of time, the connected hydro-power plant will increase production to cover the battery output and also restore the battery state-of-charge to its set-point to ready the BESS for the next deviation.

The other configuration, split frequency, is a bit different. Instead of having the battery deliver the entire frequency regulation, the frequency deviation is instead split between the BESS and the hydro-power plant, with both delivering frequency regulation. The downside to this configuration is that the HPP might still require an optimization of the control parameters in order to fulfill the demands set by the TSO.

How this is best achieved will depend on a multitude of parameters, such as: what type of turbine, installed BESS power, location of BESS in relation to the hydro-power plant as well as many others.

Between the two plants where this hybrid system has been installed, Lövön and Edsele, there are some differences. First and foremost, the capacity for the BESS at each of the locations differ as Lövön has an installed capacity of 12 MW whereas Edsele only has 9 MW.

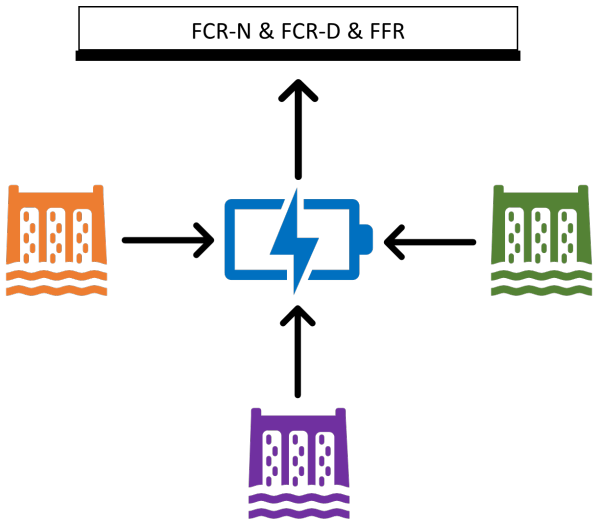

Figure 3.1: Aggregated hybrid Battery/Hydro system

Another potential configuration of this hybrid system is having one BESS connected to a multitude of HPPs and controlling them in the same way as for the single HPP, as illustrated in Figure 3.1. By sizing the BESS accordingly the owner of the HPPs can deliver FCR-N from yet more units without making any significant changes to the units.

3.1.1 Future

These types of systems, with battery energy storage systems connected to conventional production, for frequency regulation will most likely see an increase in the near future because while the cost of the system is not trivial, it does allow the access to not only the FCR-N and FCR-D markets, but also the newer FFR. As the technical requirements stipulated by the Nordic TSOs becomes stricter some of the HPPs currently participating in the frequency regulation will no longer be suited, see Section 2.2.8, unless changes are made to either the control parameters or by installing BESS. This as well as the fact that BESS are becoming cheaper, due in large part to cheaper batteries, will mean that this type of hybrid system will become more attractive.

3.2 Hydro-power plant

The worlds first hydro-electric power plant was taken online 1882 on the Fox River in Appleton, Wisconsin, USA [21] and since then, hydro-power has seen widespread use

throughout the world. In Europe, hydro-power provided 17 % out of the total production during 2018, as seen in Figure 3.2, while the corresponding number for Sweden was 39 % [22].

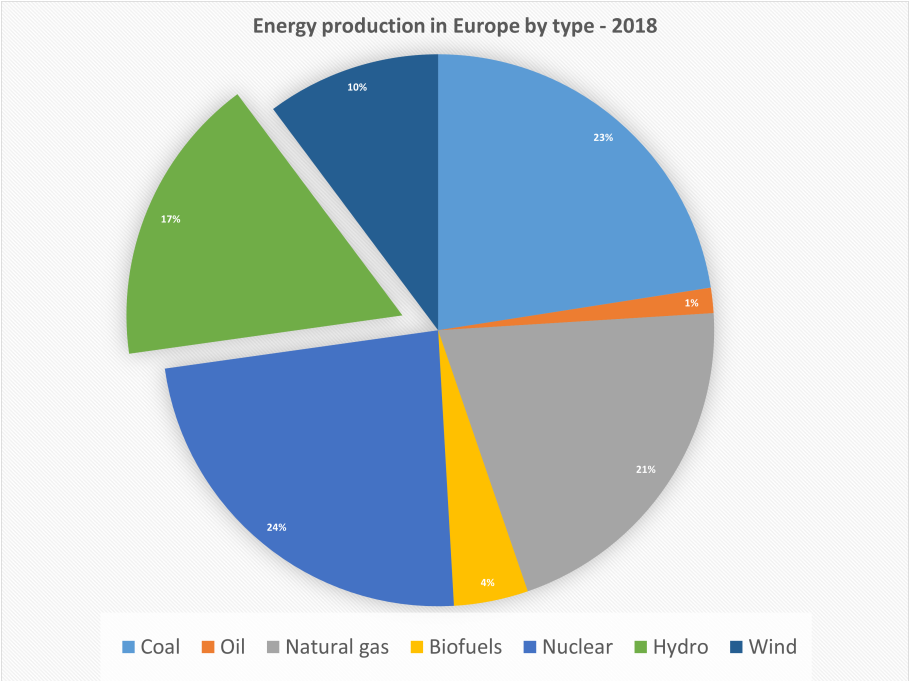

Figure 3.2: Energy production in Europe by type for the year 2018 [23]

Hydro-power is commonly used in frequency regulation as its ease of control makes it ideally suited for this, unlike wind power which in large depends on wind which can not be controlled. Contrarily, while it is easy to control, hydro-power is in general not fast enough to contribute to the added reserve type, FFR. In theory, most hydro-power plants can be optimized to allow for a faster regulation and thus fulfill the requirements for FFR, however this will increase the wear on the hydro-power system which might not be optimal. This flaw can however be mitigated by using battery storage's in conjunction with hydro-power units as this allows for a much faster injection of power into the grid while the hydro-power slowly increases the output to match the new requirement, as was demonstrated in [24].

3.2.1 Technical description

While the main concept of hydroelectric power stations has not changed since the first one was built, there are several different types of systems each with its own pros and cons. The four main ones found throughout the world are:

Impoundment hydro-power

Also known as storage hydro-power, this large system stores water in a reservoir by using a dam and generates electrical power by releasing water through a turbine. This large reservoir means that this type offers great control over production and can be used independent of rainfall and water influent during long periods. This is the most common type of hydro-power used throughout the world [25] and a great example of this type is the Hoover Dam on the Colorado River at the border between Arizona and Nevada.

Diversion hydro-power

This type diverts water from a river through a turbine which generates electrical power, and is therefore sometimes also called run-of-river or simply ROR. This type uses no (or in some cases a very small) water storage facility and is much more sensitive than the impoundment type to things such as rainfall and the waterlevel of the river. As no large dam needs to be built, they are also quite a bit cheaper which makes this type of power station popular for various small scale hydro-power applications.

Pumped storage hydro-power

A pumped storage hydro-power system is quite similar to the impoundment type, but with the possibility to pump water from a lower reservoir to a higher one when the power grid has a low demand (making the price of electricity lower). This means that by releasing water from the high to the low reservoir when there is a high demand, power is generated in the turbine and allows for the storage of energy by pumping the water back up again when there is a low demand.

Offshore hydro-power

This group is currently quite small, but has seen some growth in the last few years, and uses tidal currents or ocean waves to generate electrical power. Among the main advantages of this type is the fact that it requires practically no land for construction.

Apart from the offshore hydro-power, which uses different methods for generating electricity, all types described use the height difference between the intake and the turbine (found at a lower altitude). This height difference is denoted the gross head (H_g) and in order to simplify things the losses (mainly due to friction) are expressed as the height that corresponds to the loss, and by subtracting this height from the gross head the net head (H_n) can be calculated, as follows:

$$\begin{aligned} H_n &= H_g - H_L \\ H_g &= h_{\text{res}} - h_{\text{tail}} \end{aligned} \tag{3.1}$$

where

H_n	:	Net head	[m]
H_g	:	Gross head	[m]
H_L	:	Hydraulic losses	[m]
h_{res}	:	Reservoir level	[m]
h_{tail}	:	Tail-water level	[m]

3.2.1.1 Dam

Dams can be used to either create a reservoir or in order to divert a river, for example towards a turbine. Most modern dams are built using concrete but many different materials and construction principles are used, such as arch dams and buttress dams with the most commonly used ones being described here.

Gravity dam

A gravity dam is a large dam, usually made from concrete, designed to hold back large amounts of water in order to create reservoirs. Because of the weight of these dams they must be built on solid bedrock as to not suffer catastrophic failures. The largest dams in the world are of this type, including the worlds largest hydro-electrical dam: Three Gorges Dam in China, which is approximately 2300 metres across [26].

Arch dam

Often constructed by concrete or masonry, this type of dam is curved upstream which transfers the water pressure onto the abutments. A good example of this type is the Hoover Dam on the border between Nevada and Arizona in America, shown in Figure 3.3.

Embankment dams

An embankment dam is a large man-made dam, usually built using various materials such as soil, sand, clay or rocks and because of this they are also sometimes known as earth-filled or rock-filled dams.

Figure 3.3: Aerial overview of the Hoover Dam [27]

3.2.1.2 Waterway

The waterways of hydroelectric dams, also known as penstock or pressure shaft, are the system of pipes that brings the water from the intake gate at the reservoir to the main turbine valve. How this waterway system is constructed will depend on things such as what kind of a hydro-power plant (diversion plants sometime use a system of canals instead of pipes), height difference and length of pipe. This component, or group of components, can also include such things as surge shaft and surge tanks which are used to reduce the water hammer effects that sometimes occurs when valves are used to control the flow of liquids. This phenomenon can create immense pressure spike, sometimes exceeding ten times the working pressure, and severely damage important components, thus compromise the system integrity.

3.2.1.3 Hydraulic turbine

Turbines are generally split into two main groups; *Reaction* and *Impulse* turbines, based on how the energy conversion occurs.

Impulse turbine This type transfers the energy by using high-velocity jets directed into buckets connected to a runner wheel. The energy in the water jet is imparted onto the bucket thereby spinning the turbine while the kinetic energy of the water stream is reduced. Unlike the reaction turbine this type is therefore well suited for cases with a high head but lower flows [28].

A typical example of this type is the *Pelton* turbine, as illustrated in Figure 3.4. By alternating the amount of nozzles the turbine can be optimized for the various operational scenarios for which the *Pelton turbine* is used.

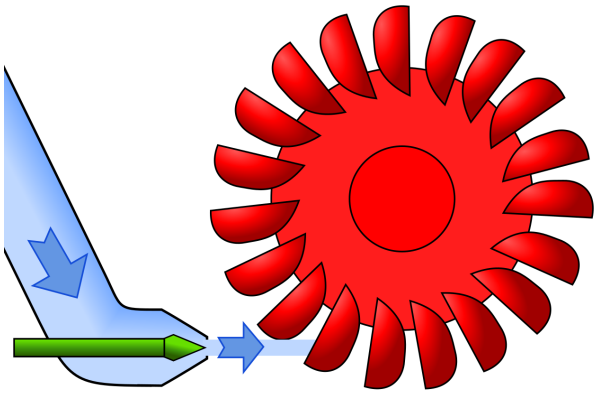

Figure 3.4: Operational principle for a Pelton turbine [29].

Reaction turbine A Reaction turbine works by reacting to the pressure or mass of a fluid, converting this into torque, according to Newtons third law which states that for every action exists a equal and opposite reaction. This group contains turbines such as the *Kaplan*, *Francis* and the *Bulb turbine* and are generally suited for cases with with lower head but higher flows.

The Kaplan turbine is a propeller type turbine with adjustable turbine blades which, in combination with inlet guide-vanes, gives a very wide flow range. The water entering the turbine housing takes a 90 degree turn, causing the water to run axial of the the runner blades, as seen in Figure 3.5. As the water strikes the blades, the turbine rotates due to the reaction force, and then exits through the draft tube. Because of the small size and high efficiency, the Kaplan is a great choice for various applications, such as diversion plants and plants with high flow rates.

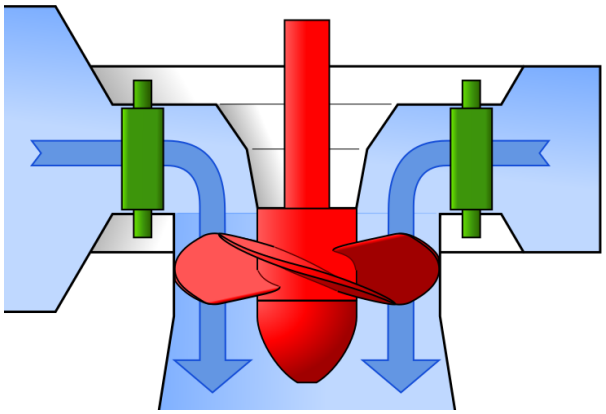

Figure 3.5: Operational principle for a Kaplan turbine [30].

The bulb turbine is, as previously mentioned, a reaction turbine and is a variation of the propeller-type (similar to the Kaplan). By mounting the turbine and generator inside a watertight housing shaped like a bulb, from where it gets its name, and mounting the whole package in such a way to allow a approximately axial flow this type allows for a lot of flexibility in powerhouse design. One drawback from this design is the added difficulty in accessing the generator and turbine for maintenance as well as the need for specialized air circulation and cooling inside the bulb. An example of how a hydro-power system using a Bulb turbine might look like can be found in Figure 3.6.

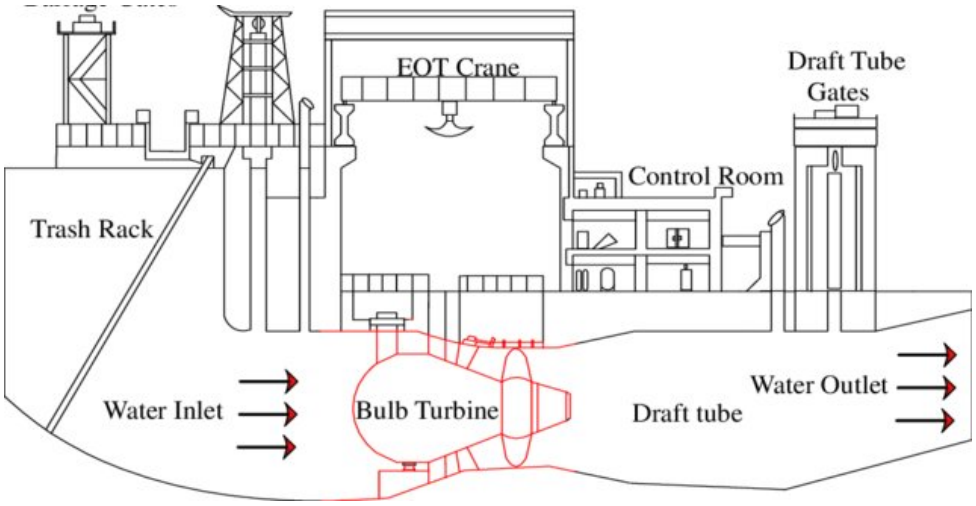

Figure 3.6: Layout example of a Bulb turbine hydro-power system [31]

For both of these turbine types, the total mechanical power available for the hydro-power plant can be described using the same equation [28]:

$$P_n = \rho Q g H_n \tag{3.2}$$

where	P_n	:	Net power	[W]
	ρ	:	Fluid density	[kg/m^3]
	Q	:	Discharge	[m^3/s]
	g	:	Gravitational acceleration	[m/s^2]
	H_n	:	Net Head	[m]

3.2.1.4 Generator

Generators are devices which convert the mechanical power from the turbine to electrical power which can be transferred to consumers via the power grid. There are two main types of AC machines found throughout the power grid; Synchronous machines and Asynchronous machines. A Synchronous machine is locked to the frequency of the grid while the Asynchronous machine operates with "slip". This slip is a percentage of how much faster, or slower, the generator rotates compared to the connected grid. Most larger power generation units are synchronous generators which, like all rotating machines, are made up of two parts; a rotating part, the Rotor, and a stationary part called the Stator.

Rotor

The rotor is essentially a large magnet, either a permanent magnet or an electromagnet, mounted on a rotating shaft. Most larger synchronous generators use the latter, an electromagnet achieved by supplying a direct current to the rotor windings, also known as the field windings, as this allows for control over reactive power and delivered voltage. The rotor shaft is in turn connected to a prime mover, i.e., the source of the mechanical power, which in the case of hydro-power systems is the hydraulic turbine.

The construction of the rotor is usually one of two types, either salient or non-salient. The salient design is typically used for larger machines with a low rotational speed (like those in hydro-power systems) whereas non-salient rotors are usually found in units with a faster rotational speed, such as those with four or less poles. [32]

Stator

The stator, or armature as it is sometimes known, is basically a hollow cylinder where vertical slots have been cut, into which the armature windings are placed. Typically the core of the stator is made up of thin sheets of silicon steel insulated on both sides to reduce eddy currents, which is one source of losses in the generator, with a stator frame outside which is designed to provide support to the core [32] [33]. As the rotating magnetic field intersects with the armature windings, three of them (each displaced by 120°) in the case of a three-phase generator, a voltage is induced.

The conversion from mechanical power to electrical power is thus described using the following equation:

$$P_{elec} = \eta P_{mech} \tag{3.3}$$

where P_{mech} : Mechanical power [W]
P_{elec} : Electrical power [W]
η : Efficiency [Dimensionless]

The voltage that is induced inside a synchronous generator will depend on various generator parameters such as the magnetic flux, rotational speed or a machine specific constant, with the resulting equation is shown in Equation (3.4).

$$E_A = K \cdot \omega \cdot \phi \tag{3.4}$$

where E_A : Induced voltage [V]
K : Machine constant [-]
ω : Rotational speed [rad/s]
ϕ : Magnetic flux [Weber]

From this it can be shown that changing either the machine constant, rotational speed or the magnetic flux will also change the induced voltage. Because the machine constant can not be changed and the rotational speed is locked to that of the grid, the induced voltage can only be regulated by modifying the magnetic flux which is accomplished by using an excitation system. The excitation system accomplishes this by varying the field current which also changes the magnetic flux.

The excitation system, which contains the AVR responsible for managing the voltage, also provides another mode which aims to keep the power factor at a constant value. This control mode is important, especially for smaller generators, because it allows the generator to produce the maximum amount of active power which, unlike reactive power, the owner gets paid for.

3.2.1.5 Control system

The hydro-power control system is in charge of managing the various functionalities used throughout the hydro-power plant and includes things such as guide-vane openings, managing the excitation system and monitoring the health of the plant. The complexity of the control system will vary as the controlled units become larger, this is because functionalities such as excitation control might be inactive for smaller hydro-power units.

While the control systems installed are usually on a per system basis, i.e., one control system per hydro-power system, they are almost always connected to an overarching SCADA system. This allows operators to control the various plants, some of which are located in remote locations, from one central control room. The control of modern hydro-power plants are usually divided into different control levels which might be located at different locations. The levels, illustrated in Figure 3.7, ranges from local individual to off-site, i.e., the regional control center.

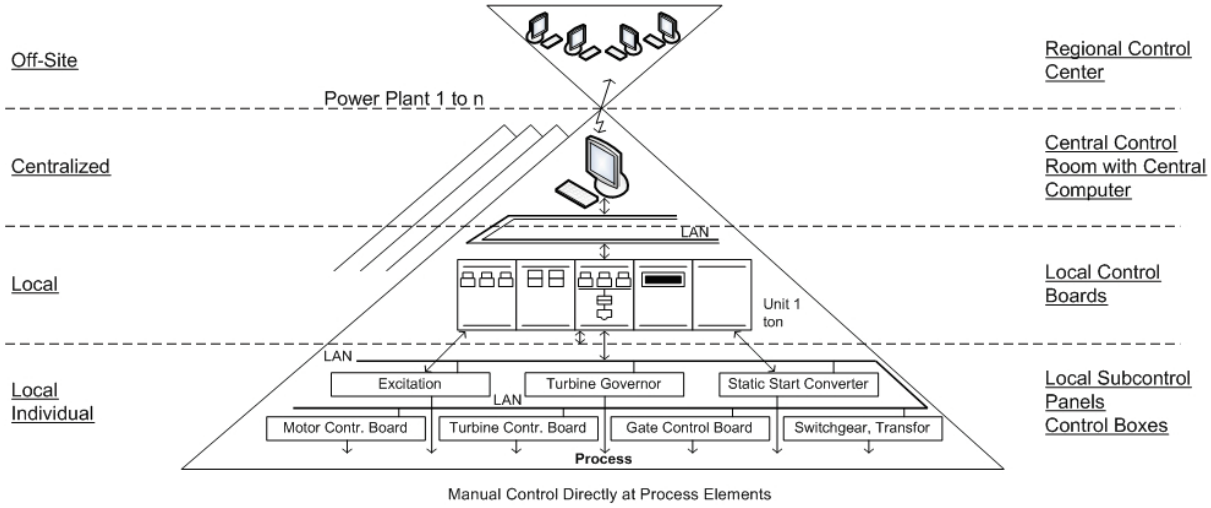

Figure 3.7: hydro-power hierarchy [34]

The actual implementation of the control system hierarchy will be different between various plants as some systems might not require a central control room and is completely controlled from off-site. This is especially true for smaller systems located in remote regions.

3.2.2 Versatility

Hydro-power systems offer a relatively high efficiency, around 95 %, and can be found with powers ranging from less than 100 kW up to 700 MW. This in combination with the

fact that turbines can be designed and optimized for a multitude of operational conditions such as high-head, low-head, low-flow and high-flow among others, means that the hydro-power system can be used in many different scenarios making it a versatile production type.

3.2.3 Sustainability

While hydro-power plants generate sustainable renewable energy while in operation, the construction of large dams (or even smaller Run-of-River plants) will impact the environment. This impact can be in the form of large scale changes, such as changing the flow of a river and resettling inhabitants, to smaller impacts, such as changing the views for people enjoying the outdoors. Beyond this, while hydro-power plants generate CO_2 during construction, they operate with very low emissions and with water-flow being the only input, the generated power is among the more clean and renewables types found in operation today.

3.2.4 Future

According to the International Energy Agency (IEA) there is a need for around 800 GW of additional hydro-power if the world is going to meet the two degrees commitment stipulated in the Paris agreement, with most of this increase expected to originate from Africa and Asia [35]. This in addition to new and interesting technologies, such as the hybrid system discussed in this Thesis, being researched will mean hydro-power remains an attractive choice in years to come.
Another interesting project is the EU funded "FRESHER", or Floating Solar Energy mooRing: Innovative mooring solutions for floating solar energy, which aims to demonstrate and validate new methods of mooring floating solar cell arrays. By installing floating solar arrays at or near hydro-power plants and using the already existing energy infrastructure a new and very interesting synergy can be developed.
In 2019 the world had a total of 1.1 GW of floating arrays installed, where the main part (450MW) is found in Asia but the technology has gathered interests in Europe as well. An example of this is the 27.4 MW project in Zwolle, Netherlands, which when fully operational will be the largest floating solar project in Europe [36].

3.3 Energy storage system

3.3.1 Technical description

The complete battery system contains many components that are needed to enable the system to work as intended. These include systems such as the battery cells, battery management system and the power management system, as well as various safety and environmental systems which are all needed to maintain a optimal operation.

There is quite a lot of variability within the existing commercial BESS found on the market today, and so the the configuration and construction will be different between the various companies. However, most complete systems use a container based construction where all the required components are fitted into a container which can then be delivered and installed on-site with ease. These containers come in many forms and shapes but one possible layout is shown in Figure 3.8 which closely resembles the ones installed at Lövön and Edsele although the described one is from a different company.

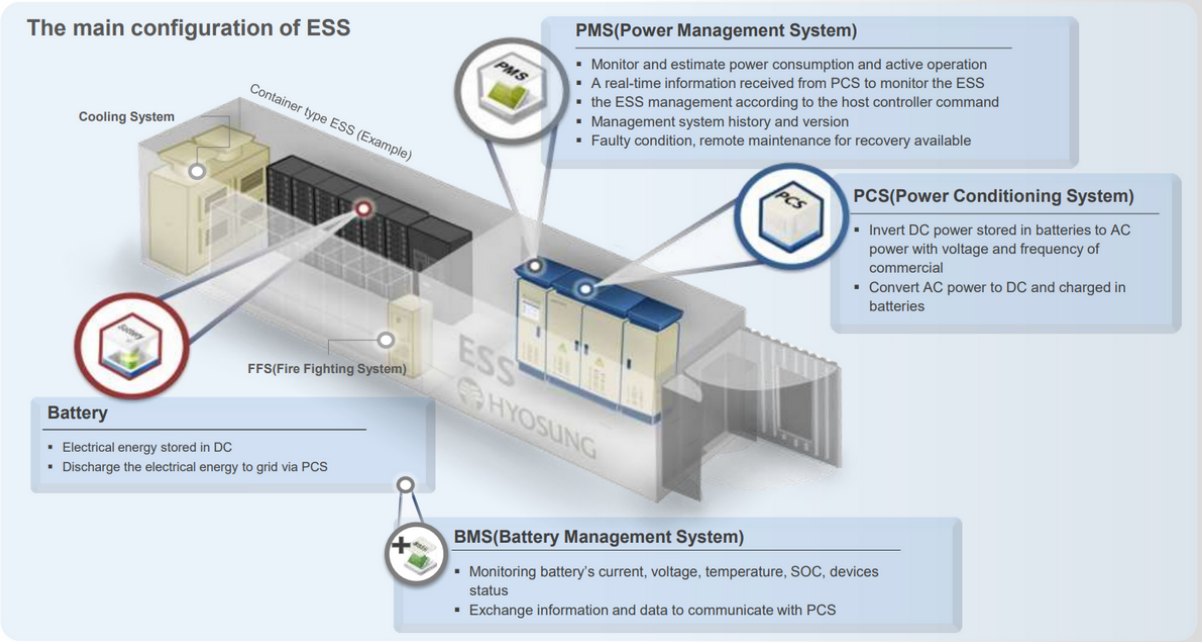

Figure 3.8: Example of a battery energy storage system [37]

3.3.1.1 Energy storage method (ESM)

Energy storage systems are fast becoming an important and vital part of the electrical grid as more and more energy is replaced with intermittent energy, such as wind and solar. There are several types of energy storage systems in use, which mainly differ in

the timescale at which they can efficiently store energy. Flywheels can store energy for several minutes up to hours, batteries up to days and pumped hydro stores energy on a seasonal timescale. These different timescales means that each of these types can find a use in the future power grid.

3.3.1.1.1 Flywheel energy storage

Flywheel energy storage works, according to the principle discussed in Section 2.2.1, by accelerating a flywheel to very high speed and storing the energy as rotational energy. The flywheel itself is essentially a heavy rotor which requires a lot of force to rotate which means that during deceleration this stored energy is released. Flywheel energy storage systems, or FESS, have seen major improvements where advanced systems are often built with rotors made from carbon-fiber composites suspended with magnetic bearings and spinning inside a vacuum. This method allows the flywheels to reach speeds ranging 20000 - 50000 rpm in a matter of minutes, therefore reaching their capacity faster than conventional flywheels.

Compared to batteries, flywheel systems are not sensitive to temperature changes, can operate in a larger range of temperatures as well as being less harmful to the environment as they contain largely inert materials. Batteries also suffer from a limited lifespan which is something that FESS does not, as these have a potentially indefinite lifespan. If conventional bearings are used instead of magnetic ones, however, the flywheel systems are subject to higher friction and might require additional maintenance.

The specific energy for a FESS will depend on two factors; The geometry of the rotor as well as the properties of the material, such as the tensile strength and density. For a rotor with a single material and a uniform geometry this can be expressed as:

$$\frac{E}{m} = K \cdot (\frac{\sigma}{\rho}) \tag{3.5}$$

where
E : Rotor kinetic energy [J]
m : Rotor mass [kg]
K : Rotor geometric shape factor [-]
σ : Material tensile strength [Pa]
ρ : Material density [kg/m3]

While flywheel systems offers a specific energy of 5-100 Wh/kg [38] with round-trip efficiencies that can reach as high as 90 % they do suffer from quite high self-discharge (3-20 % per hour) [39]. This combined with the low overall storage capacity, between 0.2 - 25 kWh, makes the FESS unsuited for long term storage of energy.

3.3.1.1.2 Batteries

Batteries are a type of energy storage that consists of one or more electrochemical cells with external connections that allow for charging and discharging. These electrochemical cells come in two versions; Voltaic and Electrolytic cells, where the voltaic cells are those which generate an electric current and electrolytic cells do the opposite, i.e., generate the chemical reactions that allow for the storing of electrical energy.

Batteries are split into various categories, mainly primary cell and secondary cell batteries, where primary cell batteries, also known as single-use batteries, are the most commonly found. These only allow for a irreversible discharge where the materials are permanently changed and are commonly found in household items such as flashlights and kitchen scales. Secondary cells on the other hand can be run as both a voltaic and as an electrolytic cell allowing for charging and discharging.

The electrochemical cells found in the secondary cell batteries are made up from two electrodes (one anode and one cathode) and an electrolyte. The electrolyte conducts the ions while blocking the electrons, which must then take the alternative route through the external circuit as seen in Figure 3.9 [40]. The materials which make up the electrolyte, anode and cathode will differ between the various battery types and have been subject to extensive research.

Each individual cell has quite a low voltage compared to the grid. For example, the reaction in a lead-acid battery cell yields only 2.04 V. This is solved by stacking cells and then connecting them either in series or parallel to each other. Connecting the cells in parallel will increase the output current while connecting them in series will increase the output voltage. Because most battery systems are sensitive to things such as temperature, voltage and current there is a need for a electronic system to manage the battery packs to ensure they do not operate outside the safe operating area. These battery management systems (BMS) also monitor the state, calculate and report various parameters and balance the cells [41].

The fact that Battery Energy Storage Systems, or BESS, offer a high energy density and a fast response time with small space requirements and no geographic restrictions (something pumped hydro suffers from) have led to an increase of these systems throughout the grid. The largest BESS currently in operation is the Buzen substation in Japan (500 MW), which uses a Sodium-sulphur battery, and the Gateway Energy Storage in the United States which is of a Lithium-ion type (230 MW). Lithium-ion is the most common battery type throughout the grid with a usage of 86.75 % [42].

There are several important parameters regarding batteries that are often used to determine the efficiency and suitability of the battery types for various tasks. No battery is ideal, meaning no losses in the actual cells, because of the internal battery resistance which generates a voltage drop during the power exchange. This means that each of the different battery types, such as Li-ion, lead-acid and sodium-sulfate, will have a different

voltage drop and therefore a different efficiency. Another parameter that differs between the types is the cyclability which is a measure of how many complete charge/discharge cycles the battery can handle before starting to break down.

Table 3.1: Percentage of total battery projects per battery type [42]

Battery type	%
Lithium-ion	86.75 %
Sodium-sulfate	8.66 %
Lead-acid	2.76 %
Vanadium Redox Flow Battery	0.52 %
Other	1.3 %

Lead-acid batteries

Invented in 1859 by Gaston Planté, the lead-acid battery is the earliest example of a rechargeable battery and is still seeing significant use because of its low cost and high power-to-weight ratio. The lead-acid batteries are built up from several lead plates arranged in parallel and alternatively polarized. The cathode plates are coated with lead dioxide (PbO_2) and the anode plates with porous lead (Pb) and both immersed into the electrolyte, which is sulphuric acid (H_2SO_4).

While lead-acid batteries are among the cheapest batteries used they do suffer from various drawbacks, such as exhibiting the poorest cyclability and a need for periodic water maintenance. Another common problem is found when the voltage used for charging exceeds recommended levels as this will cause the formation of hydrogen gas (H), which is extremely flammable.

Lead-acid batteries offer a specific energy around 35 -50 **Wh/kg** [38] which is low compared to Li-ion, but recent developments, such as bipolar lead-acid batteries, have managed a specific energy range of 55-60 **Wh/kg** [43].

Lithium-ion batteries

The lithium-ion battery usually uses a cathode made from lithium metal oxide ($LiCoO_2$) with the anode made from carbon (C). The electrolyte usually consists of lithium salts, such as $LiPF_6$, $LiBF_4$ or $LiClO_4$, suspended in an organic solution [44]. During discharging the positive lithium ions (Li^+) move through the electrolyte and the separator from cathode to anode. The electrons on the other hand, hindered by the electrolyte and the semi-permeable membrane separating the half-cells, moves through the external circuit which connects to the external load thereby providing energy [45].

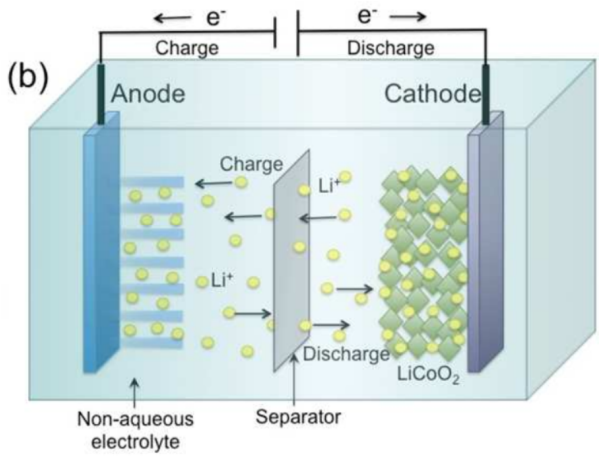

Figure 3.9: Schematic over Lithium-Ion battery [46]

The high cyclability and efficiency demonstrated by the Li-ion batteries means they are optimal for usage in combination with hydro-power, in so called hydro/battery hybrid systems, as well as in the power grid in general. Compared to the 2.04 V per individual cell that the lead-acid battery provides, the nominal voltage for the Li-ion cells are around 3.6 V with some manufacturers claiming 3.7 V and the specific energy (75-200 Wh/kg) is among the highest of the battery technologies in use today [38].

Lithium batteries do suffer from quite narrow voltage and temperature requirements which means that proper and precise measurements as well as protective circuits are required to ensure optimal operation.

Sodium-sulfur batteries

The sodium-sulfur batteries are of a relatively new type of battery technology that is showing great promise for stationary high-power applications, such as energy storage in the power grid. This type of battery is quite different compared to lead-acid and lithium-ion as these types use a liquid electrolytes with solid electrodes while the sodium-sulfate battery uses a solid electrolyte and liquid electrodes. The negative electrode, which is made up from liquid sodium, is contained inside the solid electrolyte, made from beta-alumina which is a form of ceramic aluminium-oxide. Furthermore, the solid electrolyte is encased in sulphur impregnated carbon felt which is encased in the positive electrode, which is the stainless steel can in which the entire battery is contained, as illustrated in Figure 3.10.

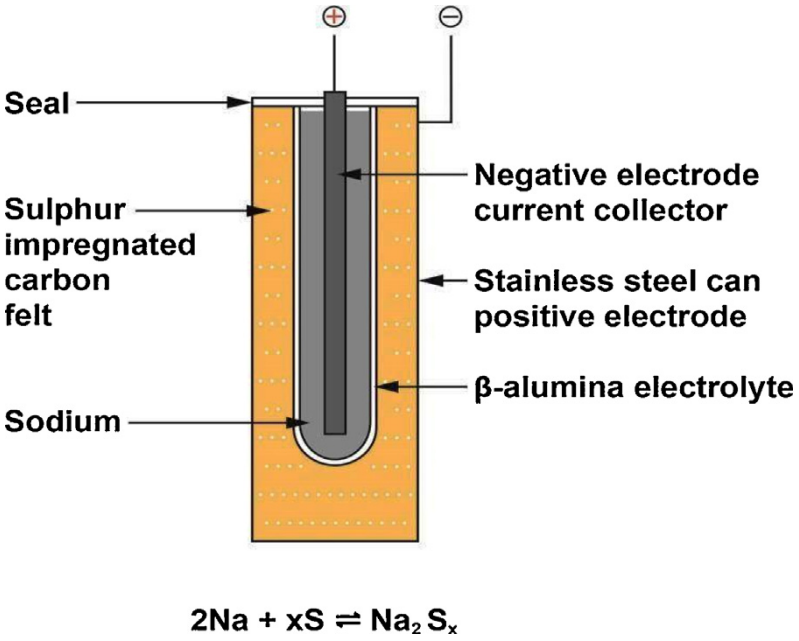

Figure 3.10: Schematic over Sodium-Sulfate battery [43]

The sodium-sulfur batteries offers high efficiency and a specific energy of 150-240 $\mathrm{Wh/kg}$ [38], which combined with the facts that this type has very low self-discharge and offers a 99 % recyclablility makes them a good alternative to lithium-ion batteries. While the sodium-sulfur batteries show low initial cost, similar to that of lead-acid, they do suffer from a few drawbacks that highlight the need for continued research and development before replacing Li-ion batteries. These problems include such things as cracking of the electrolytic tube but also corrosion due to the sulfur.

Because this type requires the sodium and sulfur to be liquid, the battery needs to operate at a high temperature of 300 °C. However, because the chemical reactions taking place are exothermic (producing heat) the required energy input for maintaining the temperature

is relatively low. As this thermal management is more costly for smaller installations, they become more economical as the installations become larger.

Flow batteries

Flow batteries, of which there are several different varieties such as vanadium redox and zinc-bromine, works according to the same principle as the previously mentioned types: The electrochemical reactions that occur inside the cells. The difference lies in the fact that the electrolyte is not permanently stored inside the cells, but rather in separate storage tanks. Increasing the size of these storage tanks therefore also increases the energy storage capacity, making this type of battery easily scalable. While flow batteries have shown to have a long lifespan and high cyclability they do suffer from low specific energy, with vanadium redox batteries ranging from 10 - 30 **Wh/kg** [38], but with proposed improvements this might potentially double, as well as increase the operational temperature range. Flow batteries are also able to full-cycle and stay at 0 % charge for longer periods of time without damage, something lithium-ion batteries are unable to do. Flow batteries, during charging, pump the fluids which contain the active materials through the electrochemical cell, causing reduction at the cathode and oxidation at the anode, and during discharge the opposite will happen. The schematic as seen in Figure 3.11 shows the operating principle of a flow cell.

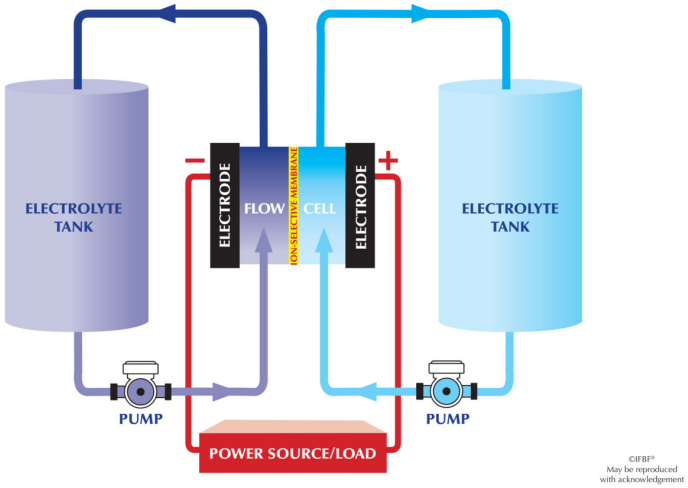

Figure 3.11: Schematic over a single flow cell [47]

3.3.1.1.3 Hydrogen energy storage

Hydrogen has been known since at least 1783, when it was named by Antoine Lavoisier [48] and has seen uses as a fuel. For example, hydrogen-based rocket fuel or early examples of hydrogen based combustion engines.

Its use as an energy storage system is, however, a fairly recent development as the interest in the technology has seen an increase due to it being identified as a key technology for the transition to a fully renewable energy system. This is, in part, because of its use in fuel-cell vehicles as an alternative to fully electric vehicles.

The main difference between using hydrogen as a storage medium and the other technologies discussed in this report is that hydrogen is quite versatile and can be used for things other than energy storage, such as steel production (as was shown in the Hybrit project [49]). While hydrogen is flammable and can be used directly in combustion engines, the best way to store energy with hydrogen is using fuel cells. Fuel cells work similarly to batteries, in which electro-chemical reactions generate electricity, but with the difference that a fuel cell requires continuous inflow of fuel (in this case hydrogen) and oxygen. In that sense, the fuel cell is quite similar to the flow batteries discussed in Section 3.3.1.1.2.

There are several ways of producing hydrogen today, with the most common way being the conversion from natural gas. This is, however, quite a carbon intense process which produces carbon dioxide as the main byproduct, which adds to global greenhouse gas emissions. However, this alternative might become more attractive as the technologies for catching and storing carbon dioxide become better and more affordable.

Currently, this problem is solved by using off-peak electricity to produce hydrogen through the electrolysis of water, which is one of the most common elements on the planet. However, while this method has seen great improvements to the efficiency, it is still relatively inefficient with around 20 % of the electricity used being lost. This might seem fairly good, but when one takes into account the fact that the conversion from hydrogen to electricity, as is done in fuel cells, has an efficiency of 60 % - the entire process is quite inefficient.

The real benefit of hydrogen, however, comes when comparing it to the current fuels used for vehicles such as diesel and gasoline. Compared to these, hydrogen has an energy density almost three times that of gasoline and diesel, making it an excellent replacement for current fossil fuels.
While fuel-cells have seen drastic improvements since their inception, they are still in their infancy with major improvements required before fuel-cell electric vehicles are a viable alternative to gasoline or diesel vehicles.

Water to energy

The concept of electrolysis (of water into hydrogen) is quite simple, albeit energy intense. By submerging two electrodes, typically made from a metal that is naturally inert (such as platinum), into water and applying a DC voltage across them hydrogen will start to appear at the cathode and oxygen will form at the anode. As water (H_2O) is made up of two hydrogen and one oxygen atom, the amount of produced hydrogen is twice that of the oxygen. This might not be true however, as there are several side reactions that occur during the process which will cause a less than ideal conversion.

The process is illustrated in Figure 3.12 where the cations represent the hydrogen molecules and the anions representing the oxygen molecules.

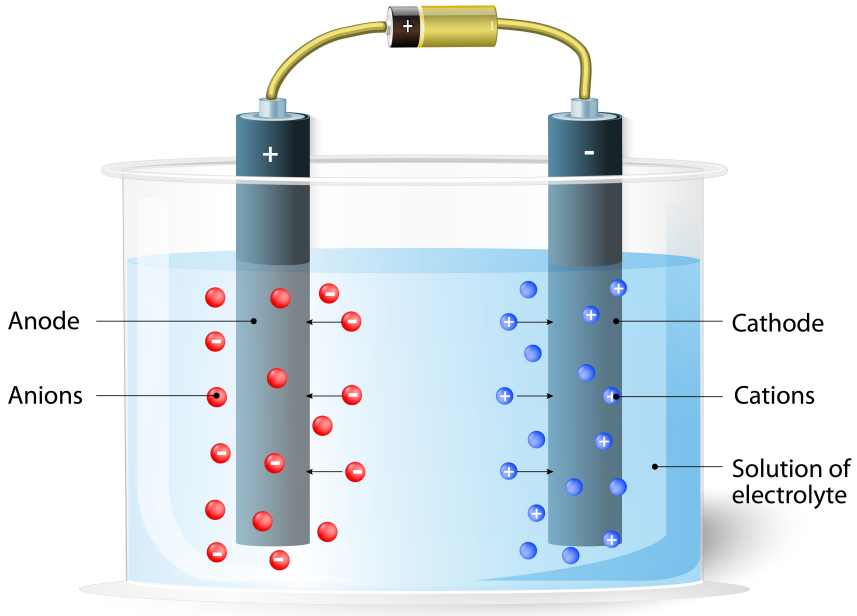

Figure 3.12: Electrolysis of water molecules [50]

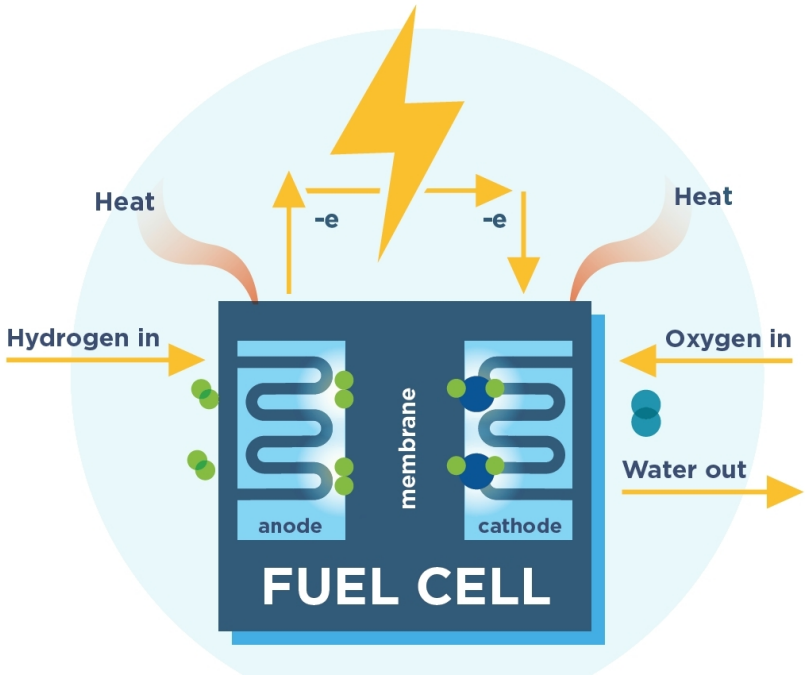

Figure 3.13: Technical diagram of hydrogen fuel-cell [52]

Energy to water

The fuel cells, much like the electrolysis equipment and batteries, consists of two electrodes. These electrodes, one being positive and the other negative, are placed around an electrolyte and hydrogen is fed to the negative electrode with oxygen being fed to the positive. The anode uses a catalyst to separate the protons and electrons in the hydrogen and forces them to take different paths to the cathode, much like for a battery, generating a flow of electricity which can then be used to power for example vehicles such as cars or forklifts. The by-product is generated by the protons reacting with the oxygen at the cathode, and is nothing more than water and heat [51].

This process, as is illustrated in Figure 3.13, is therefore very environmentally friendly as the by-products are common inert compounds that can be discharged directly into the environment.

3.3.1.1.4 System comparison

Some of the energy storage systems discussed will be better suited for different applications, one example being the flywheel. The flywheel energy system suffers from poor specific energy but instead offers among the greatest specific power out of the methods of storage discussed here. This means that the flywheel system can be found in scenarios where a lot of power needs to be delivered in a very short time. Furthermore, the flywheel energy storage systems are not that technically complex and can (in theory) last double

the amount of cycles compared to the lithium-ion batteries.

Energy storage using hydrogen might not be appropriate for the same uses as batteries, but will nonetheless be a part of the change to a more renewable and environmentally friendly power grid. However, due to this missmatch in applications hydrogen is excluded from the comparisons below.

The table below, Table 3.2, summarizes some of the most important parameters for the different energy storage systems and offer an insight in how they compare to each other.

Table 3.2: Comparison of important parameters for energy storage systems [53]

	Specific energy [Wh / kg]	Cycling times [Cycles]	Cycle efficiency [%]	Self-discharge [% / day]
Lead-acid	35 - 40	500 - 1000	70 - 80	0.1 - 0.3
Lithium-ion	100 - 200	1000 - 10000	90 - 97	< 5
Sodium-sulfur	150 - 240	2500 - 4500	75 - 90	Almost zero
Vanadium Redox	10 - 30	12000+	75 - 85	Very low
Flywheel	5 - 100	20000+	90 - 95	100

3.3.1.2 Battery management system (BMS)

The BMS is a vital part of the BESS as it is the system responsible for maintaining proper operational conditions for the batteries. This includes monitoring the various key parameters such as voltage, current and temperatures; also calculating secondary variables used for monitoring the health of the batteries, such as state-of-charge (SoC) and state of health (SoH). The BMS also handles any communication with overarching systems such as SCADA or the power management system (PMS) as well as balancing the battery cells to ensure the same SoC for each cell.

The state-of-charge calculation is done by measuring the individual cell voltages and calculating the SOC based on those voltages, but another method is by charging and discharging at constant rates via Coulomb counting. This latter version is rarely, if ever used since it adds costs and has the potential to interrupt the batteries main performance.

One of the crucial configurations for the BMS is thus the topology, as this will directly affect how the system operates and how robust it is, i.e., how resistant to disturbances the system is. Generally the topologies fall into three main categories (a fourth one, decentralized, has been proposed in various works), although the actual implementation can differ between various manufacturers. These topologies are centralized, distributed, modular and decentralized [54].

Centralized

The centralized topology is built up around having the entire BMS functionality in one single unit and connecting each of the batteries to this single unit. This means that for systems with a large amount of batteries, there will be many wires running from the cells to the BMS, something that has the potential to cause problems as it will increase the risk of short-circuit. This topology does have a few advantages over subsequent ones in that it is very cost effective and offers great accuracy as all batteries use the same offset. It is also, out of the four topologies discussed here, the least scalable with a strictly predefined limit to the number of active batteries.

Distributed

Using this topology splits the BMS into two components; The cell BMS and the BMS controller. Each battery is equipped with a cell BMS which measures the various parameters, handles battery balancing and also communicates with the BMS controller. This controller, in turn, handles the calculations of secondary variables and further communication to the connected PMS or SCADA systems.

The distributed topology offers a lot of advantages, such as an increased reliability and robustness, but the main advantage offered by this topology is the flexibility and scalability. Because there is no maximum amount of inputs, additional cells can be added after installation as long as the new modules are homogeneous. This means that the storage capacity of the system is not dependant on the BMS hardware but rather the amount of installed battery cells, which greatly increases the flexibility of the storage system.

Furthermore, due to the local control of each cell and the fact that measurements are handled at the batteries, any mandatory action needed to protect the batteries can be handled on the local level and thus increase safety. The shorter cables also means that the system is more protected against electromagnetic interference, or EMI.

All these advantages comes with a higher cost though, which is the main disadvantage for this topology, because of the need for a separate BSM is required for each battery cell as well as an additional master control module.

Modular

The modular topology can be seen as an extension to the centralized one, in that one BMS will control several batteries with the difference being in how many cells each BMS will control. Each module therefore consists of the batteries as well as the modular BMS which measures the cell voltages, currents and temperatures - as well as hosting the communication interfaces to the subsequent modules. Typical for this topology is that one BMS, either one of the modular ones or a separate BMS, will be designated as the master. This ”master” BMS is responsible for collecting the various measurements from the modules as well as controlling the entire battery pack.

A good example of this is the implementation at Lövön and Edsele, where battery modules are fitted into a rack and where each rack contains a rack BMS for control. This rack BMS is connected to the overarching SCADA system from which it takes it’s instructions.

Decentralized

The decentralized topology can be seen as an evolution of the distributed topology where the controller has been removed. Instead, the decentralization means that all of the BMS units are equal and provide the entire functionality on a local level, where the local communication interfaces offer task coordination and information exchange between the units. These communication interfaces can be more traditional, such as CAN or I^2C, or more recent ones such as wireless which would remove the risk of cable breaks.

This topology offers many advantages, such as: great scalability, improved operational security, and minimal effort in order to integrate new units, it is not without problems.

One of the biggest challenges with this topology is the fact that all these units need to work in parallel and autonomously, which can be difficult to implement in reality.

3.3.1.3 Power management system (PMS)

The power management system, hereafter referred to as PMS, is the system in charge of ensuring that the BESS delivers the power that is asked for. For frequency regulation, this means that the PMS is tasked with measuring the frequency and dispatching the required power when a deviation occurs, and in the case of Lövön and Edsele, the PMS will also send the control signal to the hydro-power plants to increase production when the deviation persists.

The PMS collects various real-time measurements (such as frequency, voltage and current) and based on these measurements calculates the secondary variables such as dispatched power and required hydro-power production.

3.3.1.4 Power conversion system (PCS)

The power conversion system, hereafter PCS, is a required component of any BESS as without this system the BESS cannot be connected to the grid. The reason behind this is that the voltage produced in the electrochemical cells of the batteries is in the form of direct current, while the grid operates using alternating current. Therefore, a converter stage is required between the batteries and the grid, which is the task of the PCS.

Because the voltages from each of the battery cells are very low compared to that of the grid, 4 V versus 4 kV, these cells need to be connected in series to produce a high enough DC voltage, typically around 600 V, that can then be converted to AC [55].

The exact operation of converting this DC to AC will depend on the configuration of the PCS, i.e., the converter topology. While the DC/AC converter is required there are also converters that use a DC/DC converter to better be able to control the voltages, as shown in Figure 3.14. There are several topologies that have been and are being used for the PCS, detailed in the sections below, and which topology is best suited will depend on a number of things [56].

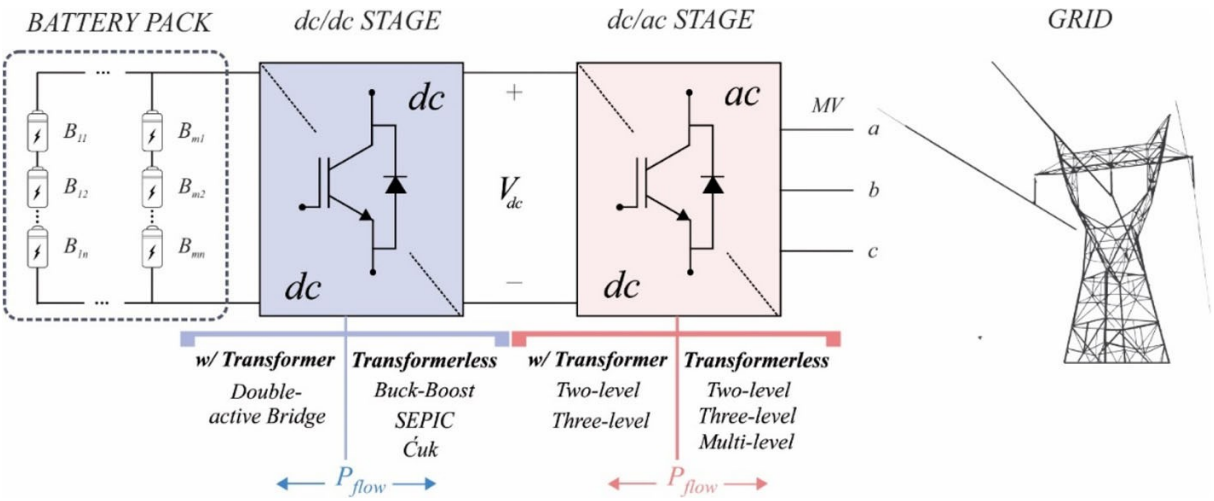

Figure 3.14: Traditional BESS structure for connection to the medium voltage grid [56]

Each topology found in PCS can be categorized into one of two types; transformer-less and with transformer. This distinction is based on whether or not a step-up transformer is required between the converter and grid. Typically, the transformer-less converters use a larger number of semiconductor devices, making them more expensive compared to those using a transformer. However, the transformer-less converters also offer a higher efficiency, and therefore lower losses, which must be considered during the planning stage of any BESS project.

With transformers

Three of the traditionally used topologies that incorporate a transformer are the voltage source converter (VSC), Z-source converter (ZSC) and the quasi-Z-source converter (qZSC). Out of these three topologies, the VSC is the simplest one and and also the most limited. The biggest disadvantage this topology has compared to the two others is that, while the batteries can be connected directly to the DC/AC converter, they can then only operate as a buck converter. This means that the output voltage must be lower than the input. Another issue with the VSC is that, because of how its set up, this converter has a larger distortion of the waveform compared to the others [56]. The Z-source converters, both ZSC and qZSC, were designed to mitigate the problems inherent to the VSC by allowing the converter to operate as a buck-boost converter without any need for a DC/DC link. This is possible due to the unique circuit configuration of the Z-source converters which use capacitors and inductors in the DC-link, as can be seen in Figure 3.15.

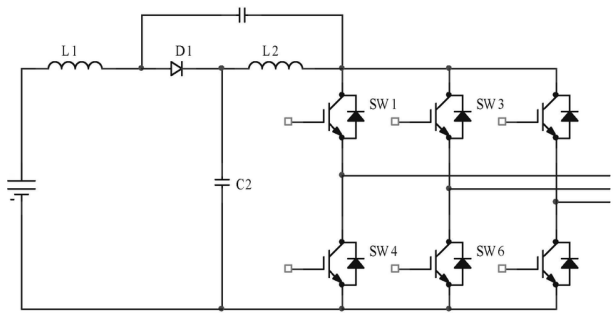

Figure 3.15: Quasi Z-Source Converter [57]

Another topology that is widely used for BESS is the NPC-, or neutral-point clamped, converter which offers several advantages, such as: lower harmonics and the possibility of higher output voltages. Compared to the VSC, ZSC and qZSC, however, this topology requires a more complex control system. Beyond the NPC converter„ there are several converters that are similar in configuration, such as the active NPC and Flying capacitor, which are described in more detail in the article by Xavier *et al* [56]. As the levels of the converters increase, from two (as for the VSC, ZSC and qZSC) towards higher levels such as the five-level NPC converters, the requirement of having a transformer is reduced as the output voltage waveform improves and the magnitude becomes higher.

Transformer-less

By using several insulated gate bipolar transistors (IGBTs) a two-level converter connected directly to the medium voltage (between 1 and 35k̃V) grid, can be achieved. The issues that come with this configuration are first and foremost the increased complexity of the gate controller, but because this converter is designed to work with a low switching frequency the requirements pertaining to filtering will increase as well.

Multi-level converters, such as the Cascaded H-Bridge converter and the modular multi-level converters with chopper or bridge cells (CC or BC), have seen an increase in discussions relating to energy storage. Figure 3.16 shows the configuration of a modular multi-level converter, which consists of n numbers of sub-modules (denoted SM in the figure) connected in series. Each sub-module is essentially a half-bridge or full-bridge converter on its own. As illustrated in the figure, each of the half-bridge modules are configured with chopper cells.

When the lower part of the half-bridge is activated the output voltage of the SM is zero ($U_{SM} = 0$), as both pins have the same potential. With the activation of the upper part, the output voltage becomes the capacitor voltage, i.e., $U_{SM} = U_{c,i}$, and the sub-module is described as *inserted*. By inserting and bypassing the the various sub-modules in a specified order and adding the voltages of the upper and lower part of the arm, a stepped sinusoidal voltage ($u_{abc,N}$) can be obtained [58].

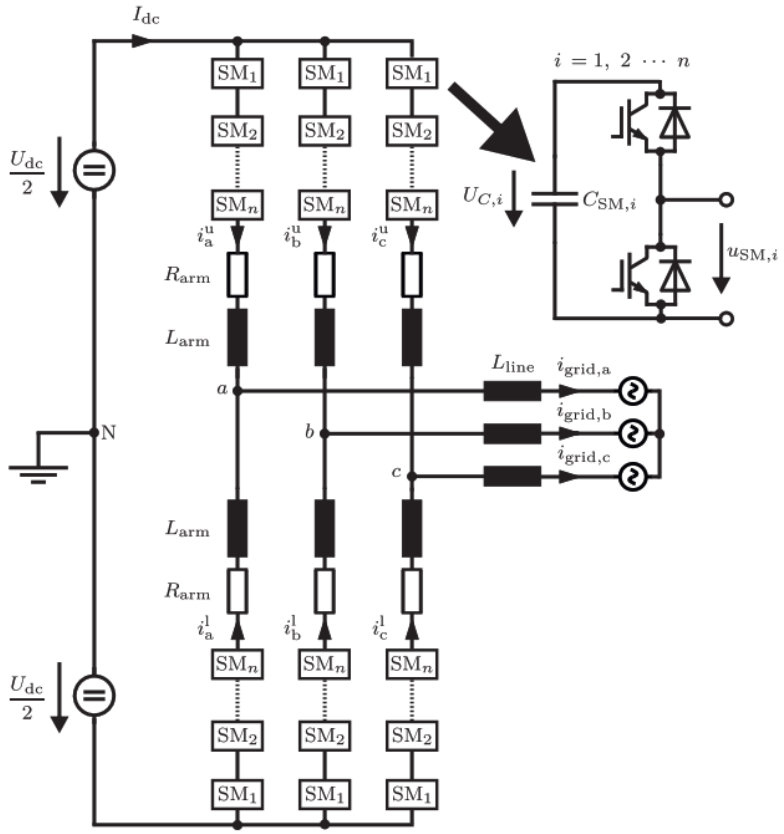

Figure 3.16: Modular Multi-level Converter (MMC) [58]

From the case study performed by Xavier *et al* [56] it was determined that while the MMC had the lowest losses as well as the higher reliability, the two- and three- level topologies are still preferable. This is due to the increase in control complexity for the MMC, as well as the fact that the two- and three-level controllers are physically simpler than the MMC. However, because of the advantages offered by the MMC there is a growing trend of using these types of converters for BESS.

3.3.2 Versatility

The two normal conditions for a hydro-power plant is synchronized and disconnected, where synchronized refers to the mode when the generator is connected to the grid and is delivering power. The other mode, disconnected, is sometimes referred to as ”island mode” and describes a scenario wherein the hydro-power plant is producing power while disconnected from the grid. During this scenario the hydro-power plant is producing enough power to balance the in-house consumption.

By installing a BESS close to the hydro-power plant, as was done in Lövön and Edsele, the operation could potentially be made more flexible by allowing charging/discharging of the BESS as needed during the disconnection. This would lessen the demands on the hydro-power units as the added storage capacity would build considerably more buffer into the system.

Photo-voltaic cells can also be installed near the hybrid battery/hydro system to allow batteries to be charged using solar power. By maintaining a state-of-charge for the BESS at 50 %, any excess power generated by the photo-voltaic cells can be sold to the grid owner without jeopardizing the main purpose of the system, i.e., to deliver FCR-N when needed.

3.3.3 Sustainability

Compared to lead-acid batteries, which because of their long history of use have a well developed recycling system built around them, lithium-ion batteries are much less recyclable. This is because, while there are collection and recycling operations found for lithium-ion batteries, the more valuable of the materials in the batteries, such as nickel(Ni), cobalt(Co) and lithium(Li), are still very hard to recycle. These materials are also among the more problematic as they are often mined in countries with little-to-no worker's rights and protections, as exemplified by cobalt. More than 70 % of the worlds cobalt supply comes from the Democratic Republic of Congo, which for years has seen documented issues with human rights, as observed by Amnesty International and the United Nations. This means that each company in the logistics chain regarding lithium-ion batteries have a responsibility to ensure that the ore has been mined in a sustainable and eco-friendly way, without issues regarding human rights.

As the demand for batteries will only increase - with the world moving towards a more electrified society - the need for proper recycling will increase as well. The increased interest in lithium-ion batteries that has taken place during the last decade does not extend only to research into better batteries, but also into how to better recycle and reuse those batteries. A study performed by Circular Energy Storage, a London-based consulting firm, in 2019 shows that the number of published articles regarding recycling of lithium-ion batteries saw an increase of more than 300 % between 2015 and 2018 [59].

3.3.4 Future

The research and development into batteries has increased rapidly, driven in part by the electrification of vehicles and increasing percentage of intermittent production. This has led to a decrease in price as the energy density of batteries increases. Over the

past 10 years lithium-ion prices have decreased by approximately 85 %, as illustrated in Figure 3.17, which is based on the survey performed by BloombergNEF in 2019 [60].

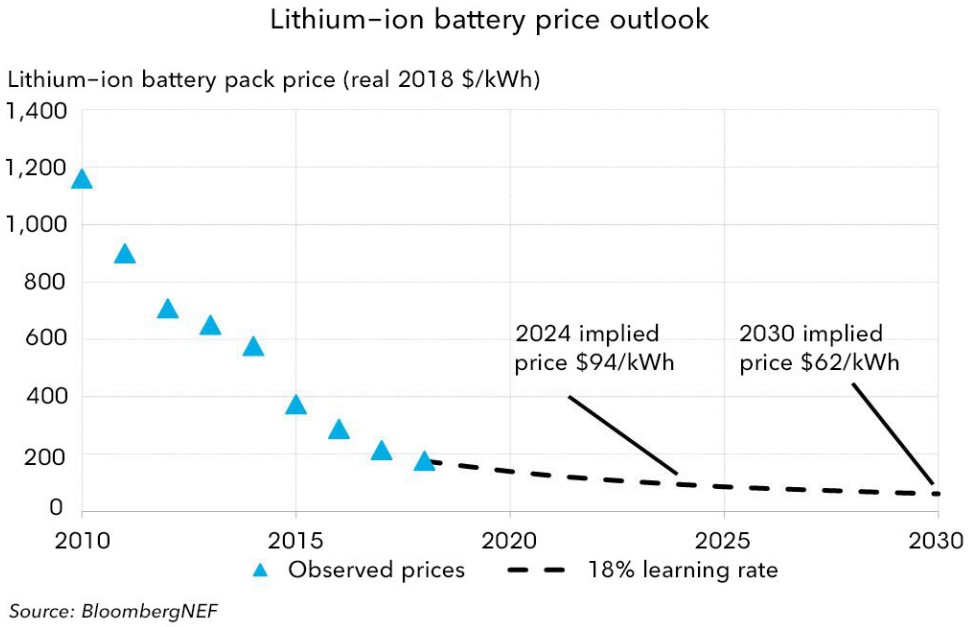

Figure 3.17: Average Lithium-ion battery pack price per kWh since 2010 [60]

One of the main advantages that BESS has over - for example, pumped hydro storage is that while PHS generally have a higher storage capability, they are not easily upgraded. This is unlike BESS, which offers a relative ease of capacity increase. This means that as the technologies mature and become cheaper, the plants with already existing BESS installations can be updated to ensure the optimal technology is used.

Among the various battery technologies being researched, the solid-state battery has shown great promise. This type of battery uses both a solid electrolyte and a solid electrode which offers many pros over conventional types. These pros include the potential of making the batteries safer as well as making them capable of higher energy densities. These pros are balanced, however, by the increased cost compared to matured battery technologies such as the conventional Li-ion.

4 Modelling

In order to provide a test-bed for various configurations and simulations of the implemented system, a model was built in MATLAB/Simulink. The model is based on previous work and has seen use in previous studies regarding primary frequency control [61][62] as well as hydro/battery hybrid systems [19]. The simplified model is used to simulate how the Nordic grid, the connected FCR-N units and the hydro/battery hybrid system (HBHS) will react to a simulated production loss.

The complete model is split into various components such as the Nordic power grid model, The lumped production model and the HBHS model. All models will use a per-unit system to simplify calculations, with the defined base values as seen in Table 4.1.

Table 4.1: Simulation per-unit base values

Parameter	Base value
Frequency	50 Hz
Active power	37 650 MW

4.1 Nordic power grid model

When an imbalance between production and consumption occurs, the frequency will deviate based on the system inertia and the system damping. The system inertia is a description of the amount of stored kinetic energy found throughout the grid whereas the system damping describes the various frequency dependant loads in the grid, which will reduce or increase their consumption when the frequency starts to deviate.

During a frequency deviation in the grid all the connected rotating machines will react to the deviation, either by absorbing excess energy or by providing energy. This will accelerate or decelerate the machines according to Equation (4.1), also known as the swing equation.

$$J_i \omega_i \frac{d\omega_i}{dt} = P_{\text{mech}_i} - P_{\text{electrical}_i} = \Delta P_i \tag{4.1}$$

where J_i : Machine inertia [kgm^2]
ω_i : Machine angular speed [rad/s]
P_{mech_i} : Driving mechanical power [W]
$P_{\text{electrical}_i}$: Braking electrical power [W]

The angular speed of the machine and the moment of inertia will also determine the amount of stored kinetic energy in the machine, as described by Equation (4.2).

$$E_{\text{kinetic}_i} = \frac{1}{2} J_i \omega_i^2 \tag{4.2}$$

where E_{kinetic_i} : Machine kinetic energy [J]

By inserting the equation for kinetic energy into the swing equation and equating the grid frequency to the machine speed a generalized equation describing the correlation between production, consumption and system inertia is determined as Equation (4.3).

$$\begin{aligned} J_{\text{sys}} \frac{d\omega_g}{dt} &= P_{\text{prod}} - P_{\text{cons}} \\ J_{\text{sys}} &= 2\frac{E_{\text{kin}}}{\omega_s} \end{aligned} \tag{4.3}$$

where P_{prod} : Total system production [W]
P_{cons} : Total system consumption [W]
J_{sys} : Total system inertia [J]

The damping of the system describes how certain loads will change when the frequency change, which means that these types of loads will assist in stabilizing the grid when frequency deviations occur. The system damping is therefore a measure of this reduction and is described by Equation (4.4).

$$D = \frac{\Delta P_{\text{cons}}}{\Delta f} \tag{4.4}$$

where D : System damping [MW/Hz]
ΔP_{cons} : Change in system consumption [W]
Δf : Change in system frequency [Hz]

From Equation (4.3) and the equation for the frequency dependant loads, the final transfer function in the Laplace domain, which is then implemented in Simulink, is obtained and described in Equation (4.5).

$$\Delta f(s) = \frac{1}{J_{\text{sys}}s + D}\Delta P \tag{4.5}$$

4.2 Hydro-power production model

Hydro-power units participating in the FCR-N market work by reacting to frequency changes by either increasing or decreasing the production according the to the droop principle, as shown in Figure 4.1. Simply put, with a decreasing frequency (illustrated by the dotted red line) the produced active power will increase and vice versa.

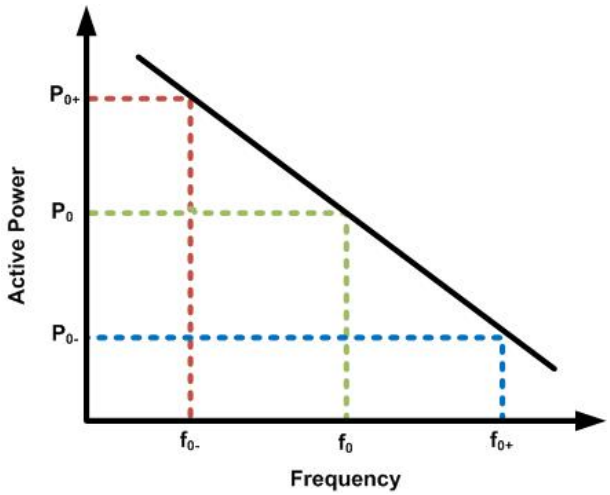

Figure 4.1: Conventional droop characteristic [63]

The entire FCR-N capacity in the Nordic grid will be simulated using a lumped parameter model, similar to those used by Danilo Laban [19] and Linn Saarinen *et al* [61].

The model for the hydro-power production units consists of models for the hydraulic and mechanical subsystems as well as a model representing the standard turbine governor used throughout Sweden, which is a closed-loop PI controller with droop. While the droop setting defines the control loop static gain, the PI controller will ensure that no steady state error remains. Typically, Swedish hydro-power units use the guidevane position as the feedback variable, although it is possible to use the active power as feedback, due to the increased stability margins offered. Due to this, the model used throughout this Thesis will use the guidevane opening as the feedback variable.

The droop setting used by most hydro-power units in the Nordic grid, usually referred to as the Ep setting, is thus defined as:

$$E_p = \frac{\Delta f}{\Delta P_{\text{prod}}} = \frac{\Delta f}{\Delta Y} \tag{4.6}$$

The error signal (e_f) is generated by subtracting the reference value(50 Hz) and the droop position feedback($E_p \Delta Y_{\text{meas}}$) from the measured frequency(f_{meas}), this gives the error signal described as:

$$e_f(s) = f_{ref} - f_{\text{meas}}(s) - E_p \Delta Y_{\text{meas}}(s) \tag{4.7}$$

This error signal is then passed through a low-pass filter, with the time constant $T_{meas-filter}$, that suppresses the measurement noise inherent in the frequency measurements before being forwarded to the PI-controller.

By limiting the PI-controller output, so as to not allow a production higher than the allotted FCR-N capacity, the calculated guidevane reference signal in the Laplace domain is defined as:

$$\Delta Y_{\text{ref}} = \left(K_p + \frac{K_i}{s} \right) \cdot \frac{1}{T_{\text{meas-filter}} s + 1} \tag{4.8}$$

where

ΔY_{ref}	:	Guide vane reference	[pu]
K_p	:	Proportional gain constant	[pu]
K_i	:	Integration gain constant	[pu]
$T_{\text{meas-filter}}$	:	low-pass filter time constant	[s]

With the output limited to $\pm \Delta Y_{\max}$ when the frequency deviation exceeds the maximum value, usually 0.1 Hz, it is passed to a model representing the servo system. The dynamic response of the servo is modelled after a full-scale test performed at three hydro-power plants in Sweden [64] where the behaviour of the servo system was determined to be a first-order lag, with the time constant T_y and a time delay ($T_{\text{delay-y}}$). The servo behaviour in the Laplace domain is therefore described as:

$$\Delta Y_{\text{meas}}(s) = \frac{1}{T_y s + 1} e^{-s T_{\text{delay-y}}} \Delta Y_{\text{ref}}(s) \tag{4.9}$$

where

ΔY_{meas}	:	Measured guide vane position	[pu]
T_y	:	Guide vane time constant	[s]
$T_{\text{delay-y}}$	:	Guide vane time delay	[s]

As the hydro-power units used at Edsele and Lövön are Kaplan and Bulb turbines respectively, the servo model needs to be extended. This is because, while a Francis turbine

governor only controls the guide vanes, the Kaplan and Bulb controllers also regulate the runner vanes. This is modelled using the same approach as the guide vanes, i.e., a first-order lag with a time delay, with the measured guide vane opening used instead of the reference value from the PI-controller.

$$\Delta A_{\text{meas}}(s) = \frac{1}{T_a s + 1} e^{-sT_{\text{delay-a}}} \Delta Y_{\text{meas}}(s) \tag{4.10}$$

where
ΔA_{meas} : Measured runner vane position [pu]
T_a : Runner vane time constant [s]
$T_{\text{delay-a}}$: Runner vane time delay [s]

Another effect which occurs in hydro-power units and which therefore must be included in the model is the backlash effect. This effect describes the empty movement that occurs during regulation where the physical position of the mechanical parts are offset from the position measured by the governor. This backlash is applied to both the guide vanes as well as the runner vanes and can be described as a floating hysteresis around the guide vane position. Including this backlash effect into the model yields the variables ΔY_{pos} and ΔA_{pos} and the finalized model describing the turbine governor and servo system for a Kaplan turbine, shown in Figure 4.2.

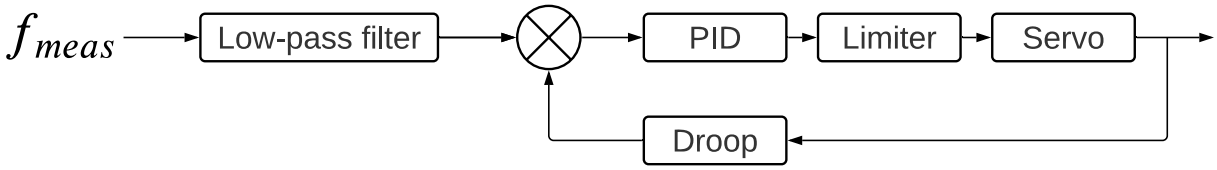

Figure 4.2: Finalized model describing the turbine governor and servo

The next step is to model the hydraulic system as well as the water dynamics to obtain produced mechanical power. Based on earlier work, the model used is a non-minimum phase first-order with the water time constant T_w [61].
The hydraulic model for a Kaplan turbine, which takes the guide vanes and runner vanes into account, is thus given in Equation (4.11).

$$\Delta P_{\text{prod}}(s) = \frac{-T_w s + 1}{0.5 T_w s + 1} [K_y \Delta Y_{\text{pos}} + K_a \Delta A_{\text{pos}}] \tag{4.11}$$

where
ΔP_{prod} : Produced mechanical power [pu]
T_w : Runner vane time constant [s]
ΔY_{pos} : Guide vane position (backlash included) [pu]
ΔA_{pos} : Runner vane position (backlash included) [pu]
K_y : Guide vane contribution factor [pu]
K_a : Runner vane contribution factor [pu]

With this, the model describing the hydro-power unit is complete and the final structure is shown in Figure 4.3. Furthermore, the model parameter values are displayed in Table 4.2.

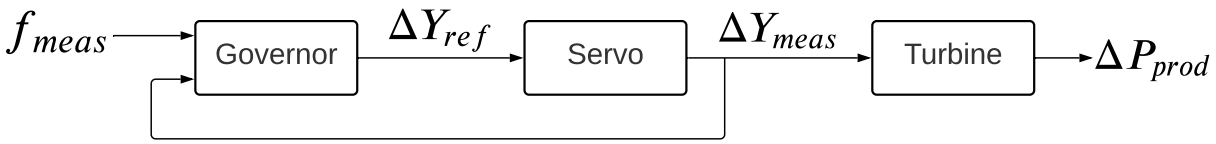

Figure 4.3: Finalized model describing the hydro-power production unit

Table 4.2: Hydro-power unit parameter values

Parameter	Symbol	Value	Unit
E_p	Droop constant	0.1	pu/pu
K_p	Controller proportional gain	1	pu
K_i	Controller Integral gain	1/6	pu
$T_{\text{meas-filter}}$	Frequency measurement filter time constant	2	s
T_y	Guide vane servo time constant	0.2	s
$T_{\text{delay-y}}$	Guide vane servo time delay	0.3	s
T_a	Runner vane servo time constant	1	s
$T_{\text{delay-a}}$	Runner vane servo time delay	0.5	s
T_w	Water time constant	1.5	s
K_y	Kaplan guide vane contribution factor	0.3	pu
K_a	Kaplan runner vane contribution factor	0.7	pu
Bl_y	Guide vane backlash	0.1	%
Bl_a	Runner vane backlash	0.2	%

In order to properly simulate the hybrid system, a model representing a single hydro-power unit must be defined. This is done by having the lumped production model represent *n-1* units in the grid and having the hybrid system model represent the remaining unit. The result is one separate model for the hybrid system and another model that represents the remaining units participating in FCR-N. This is accomplished by modifying the droop

constants of the units by introducing a scaling ratio (K_h) based on the size of the single hydro-power unit compared to the rest of the system, i.e.,

$$K_h = \frac{R_h}{R_{\text{FCR-N}}} \tag{4.12}$$

which is then used to modify the parameters used for the two units, lumped and single.

Therefore, by multiplying the parameter values found in Table 4.2 by K_h for the single unit and by $1-K_h$ for the *n-1* unit, the model is now ready to simulate both the dynamics of the single unit as well as lumped production unit with the new values.

4.3 Historical disturbance model

While detailed historical data regarding the measured frequency of the grid is provided by Fingrid, this data needs to be converted into a power disturbance before being used in the simulations.

However, the frequency data also contains information about the FCR units which were active during the measurement period. Apart from inverting the grid model, this contribution needs to be removed so as to reconstruct the power deviation that leads to the corresponding frequency. The measured frequency, sampled at 0.1 seconds, is fed into the model representing the lumped production (see Figure 4.3) and the inverted grid model. By inverting the grid model and adding the historical power production, the historical disturbance model is defined in Equation (4.13) with the structure illustrated in Figure 4.4.

$$\Delta P_{\text{hist}} = \frac{Ms+D}{T_{ff}s+1}\Delta f_{\text{hist}} + \Delta P_{\text{prod}} \tag{4.13}$$

where	M	:	Total system inertia	[J]
	D	:	System damping	[MW/Hz]
	T_{ff}	:	Low-pass filter time constant	[s]
	ΔP_{prod}	:	Historical FCR-N contribution	[pu]
	Δf_{hist}	:	Historical frequency	[pu]

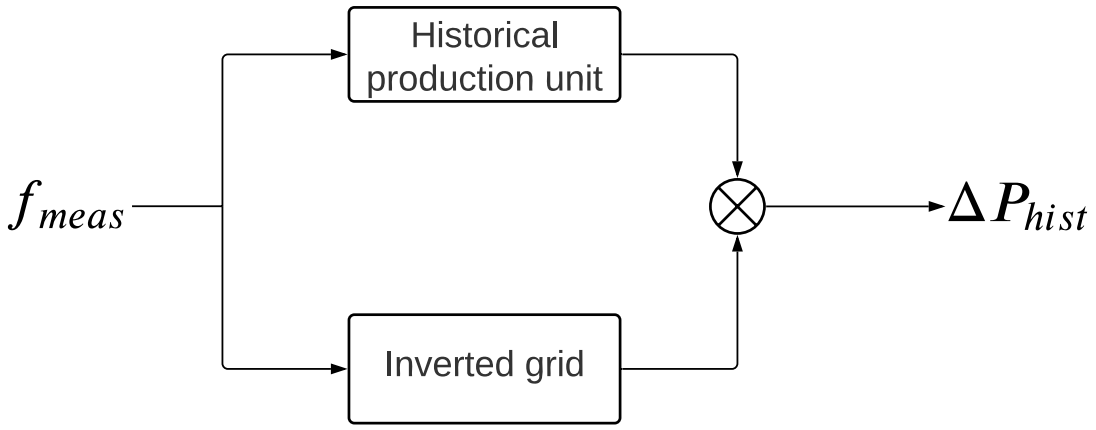

Figure 4.4: Final model structure of the historical disturbance model

4.4 Battery energy storage model

Because the dynamic behaviour of the BESS is mainly dependant on the chemical and electrical subsystems, as explained in Section 3.3, the model will be composed of models representing the power control and the electrical subsystems. The power control belongs to the power plant controller and will thus be described in the following section, while the electrical subsystem of the BESS is described in this section.

The behaviour of the electrical subsystem is modelled using a first-order lag with a time constant(T_{bess}) and a time delay($T_{delay-c}$) based on values taken from the documentation provided by Uniper.

The BESS active power output can thus be described as follows:

$$\Delta P_{\text{BESS}} = \frac{1}{T_{\text{bess}} s + 1} e^{-sT_{\text{del-c}}} \Delta P_{\text{BESS-ref}} \tag{4.14}$$

where

$\Delta P_{\text{BESS-ref}}$	:	BESS active power reference	[pu]
ΔP_{BESS}	:	BESS active power output	[pu]
T_{bess}	:	BESS time constant	[s]
$T_{\text{delay-c}}$	:	Bess time delay	[s]

Beside this, the BESS model also needs to calculate the state of charge, which is simply done by integrating the output over time. So, as the model is discharging the state of charge is decreasing and vice versa, giving an accurate reading of the current BESS state of charge at all times. This is described by the following equation, which assumes that there are no losses when charging/discharging:

$$\text{SoC}(s) = \frac{1}{s} \Delta P_{\text{BESS}}(s) \tag{4.15}$$

While this assumption is not correct, it is deemed accurate enough since focus is on the hydro-power units and not the BESS. However, this should be amended in future model improvements.

4.5 Power plant controller

The power plant controller is in charge of dispatching the required power from the BESS during a frequency deviation and ensuring that the hydro-power unit ramps up to compensate during longer periods of deviation. The model is based on documentation about the actual units implemented at Lövön and Edsele, received from Uniper. However, due to the information given being quite sparse (because of confidentiality) the model will not be an exact copy.

The controller is made up of three sub-controllers, as can be seen in Figure B.1 which describes the structure of the power plant controller. Due to reasons regarding confidentiality, however, these are not made public. Furthermore, due to the limited scope of this Thesis, the state-of-charge controller has been omitted from the model, with focus instead being on the reduced wear and tear on the turbines. The two remaining controllers; frequency services and the distributor, are described in greater detail in the subsequent sections.

Frequency services

While the actual installed unit provides the possibility to deliver not only FCR-N but also FCR-D UP and FFR, these last two services are deemed to be out of the scope of the simulation and are therefore omitted. The calculation for the frequency set-point is relatively straight forward, with only a time constant (T_{FCRN}) and a proportional gain (K_{p-FCRN}). Beside this, the frequency input is also filtered and limited, much like for the hydro-power unit, to ensure that only the power dedicated to the FCR-N is delivered.

The required power dispatch is thus described as:

$$\Delta P_{\text{BESS-ref}} = (K_{\text{p-FCRN}}) \frac{1}{T_{\text{FCRN}}} \Delta f_{\text{meas}} \tag{4.16}$$

where

Δf_{meas}	:	Measured frequency deviation	[pu]
$\Delta P_{\text{BESS-ref}}$	:	BESS active power reference	[pu]
$K_{\text{p-FCRN}}$	:	BESS proportional gain	[pu]
T_{FCRN}	:	BESS time constant	[s]

Distributor

The active power reference that is passed to the hydro-power units is based on the sum of the required dispatched power, which consists of the FCR-N dispatch and state-of-charge manager outputs, as well as the power ratings of the connected hydro-power units.

Therefore, the calculated reference power can be described with the following equation:

$$P_{\text{G1-SP}} = P_{\text{FCR-SP}} + P_{\text{SOC-SP}} \tag{4.17}$$

where
$P_{\text{G1-SP}}$: Generator 1 Active power set-point [pu]
$P_{\text{FCR-SP}}$: Frequency services active power set-point [pu]
$P_{\text{SOC-SP}}$: State-of-charge manager active power set-point [pu]

This reference power is then split between the connected hydro-power units and passed to a stateflow chart which discretizes the signal into a signal composed of block steps with a specific duration and a specific magnitude, values taken directly from the documentation. This functionality is described in Figure 4.5, which shows the output of the block generator when a step signal is used as input. By comparing the stateflow chart input to the output, the correct state can be activated thereby either increasing or decreasing the output until they are equal or until the input signal changes. When the output is equal to the input, the *idle* state is activated as no more actions are needed from the stateflow chart.

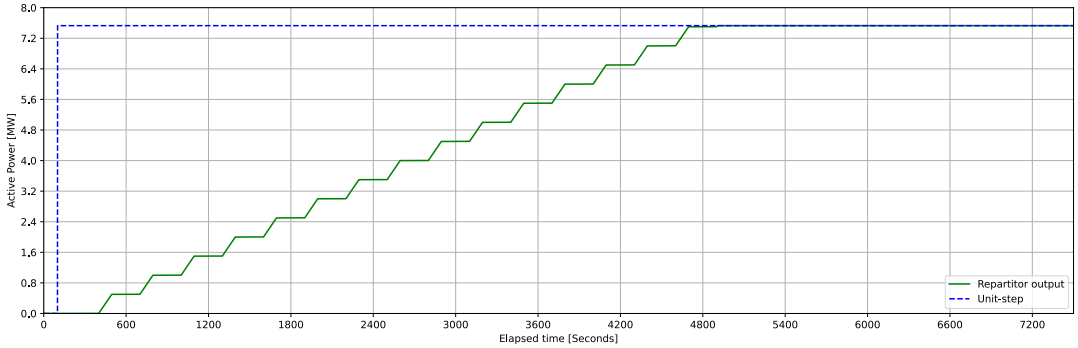

Figure 4.5: Example of quantizer output.

Furthermore, both of the changing states work the same way, by first altering the output by the chosen step height and then holding that value for the set amount of time. If the output suddenly becomes larger than the input, the activated state changes from *increase* to *decrease* and vice versa if the output suddenly becomes smaller than the input. Each of the two states has three sub states, as seen in Figure 4.6, which describes if the output signal is holding, changing or if its the final change before output and input are equal. The logic behind the transitions between these states should be evident from the figure,

but essentially as soon as the block time has elapsed the block height is compared to the remaining error between the input and output. If this remaining error is larger than than the block height the output is increased / decreased by the block height, otherwise the output is increased / decreased by the remaining error as this is the last increment before entering the *idle* state.

This gives a stateflow chart with the following structure:

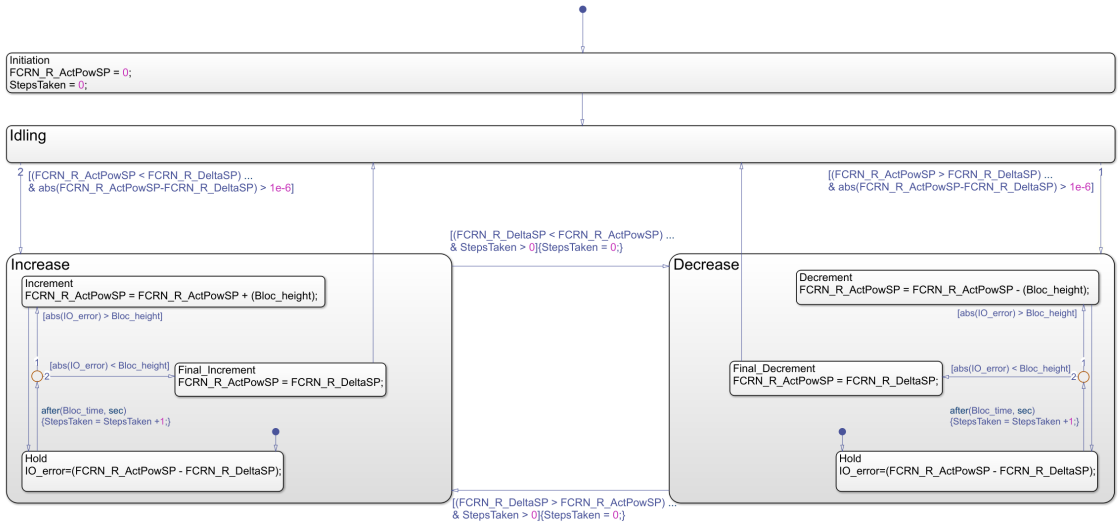

Figure 4.6: Implemented Simulink stateflow chart

4.6 Wear and tear calculations

The regulation wear and tear of hydro-power units due to the constant changes of the frequency is an important parameter that needs to be investigated when comparing two systems, such as one with BESS and one without.

In order to quantify the wear and tear which the hydro-power units suffer, two key process indicators (KPI) are used; guide/runner vane distance and number of movements. This is the same as was done in previous research [61][19], providing an opportunity for comparing the results and verifying the model.

By integrating the position change (derivative of the absolute position) over the simulation time, the total distance travelled by the vanes are calculated, as described by:

$$L_{\text{wt}} = \int_0^{T_{\text{sim}}} d|\Delta Y_{\text{meas}}| \tag{4.18}$$

where L_{wt} : Distance travelled by vanes [pu]
T_{sim} : Simulation time [s]
ΔY_{meas} : Measured vane position [%]

This is implemented in MATLAB/Simulink according to the structure as illustrated in Figure 4.7, which consists of blocks representing the functions integration, derivative and absolute value.

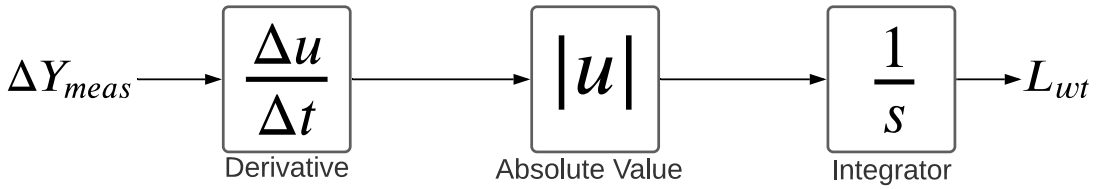

Figure 4.7: Model of the vane distance calculation

For the second KPI, vane movements, the implementation is not as straight forward. The simplest implementation would be to count the number of times the vanes come to a complete standstill, i.e., when the derivative of the position equals zero. however, this approach is problematic for two reasons: Matlab (as with any numerical environment) has problems evaluating the value zero and the vanes rarely come to a complete stop.

Both of these issues can be solved by introducing a tolerance (ε_{wt}) and defining a movement as any time the vanes have moved less than the tolerance during the specified sampling time (T_{wt}). Furthermore, the introduction of a floating hysteresis can serve to limit the simulated movements dependency on the chosen value of the tolerance.
This approach was put forward by Danilo [19] and is also used here. With this, and by implementing a counter that increments on the rising edge of the inequality, the final algorithm can be defined as:

$$N_{\mathrm{wt}} = \begin{cases} +1, & |\Delta Y_{\mathrm{wt}}(t) - Y_{\mathrm{wt}}(t - T_{\mathrm{wt}})| > \varepsilon_{\mathrm{wt}} \\ 0, & |\Delta Y_{\mathrm{wt}}(t) - Y_{\mathrm{wt}}(t - T_{\mathrm{wt}})| < \varepsilon_{\mathrm{wt}} \end{cases} \tag{4.19}$$

where N_{wt} : Number of movements [Dimensionless]
ΔY_{wt} : Measured vane position with hysteresis [%]
T_{wt} : Specified time delay [s]
$\varepsilon_{\mathrm{wt}}$: tolerance [pu]

The values used for the parameters: T_{wt}, ε_{wt} as well as the implemented hysteresis (Bl_{wt}) are the same as used in the previous research which this work is based on. This is to ensure consistency and allow for comparisons between the different simulations. The finalized

structure in Simulink is thus illustrated in Figure 4.8 below, with the parameter values presented in Table 4.3.

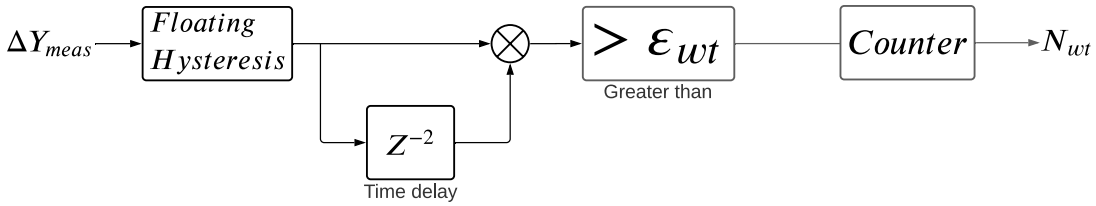

Figure 4.8: Model of the vane movement calculation

Table 4.3: Wear & tear parameter values

Parameter	Value
$\mathrm{Bl}_{\mathrm{wt}}$	$2\mathrm{Bl}_y$
$\varepsilon_{\mathrm{wt}}$	$5\mathrm{Bl}_y$
$\mathrm{T}_{\mathrm{sim}}$	2 [s]

4.7 Simulation scenario

In total, two simulations were performed with one representing the case when all FCR-N is delivered strictly from hydro-power units and the second one containing the hybrid system. The former case will thus contain models describing the single Kaplan, lumped production and Nordic power grid (all of which are described in Chapter 4), while the latter case includes the hybrid system instead of the single Kaplan as illustrated in Figure 4.9 and Figure 4.10 respectively.

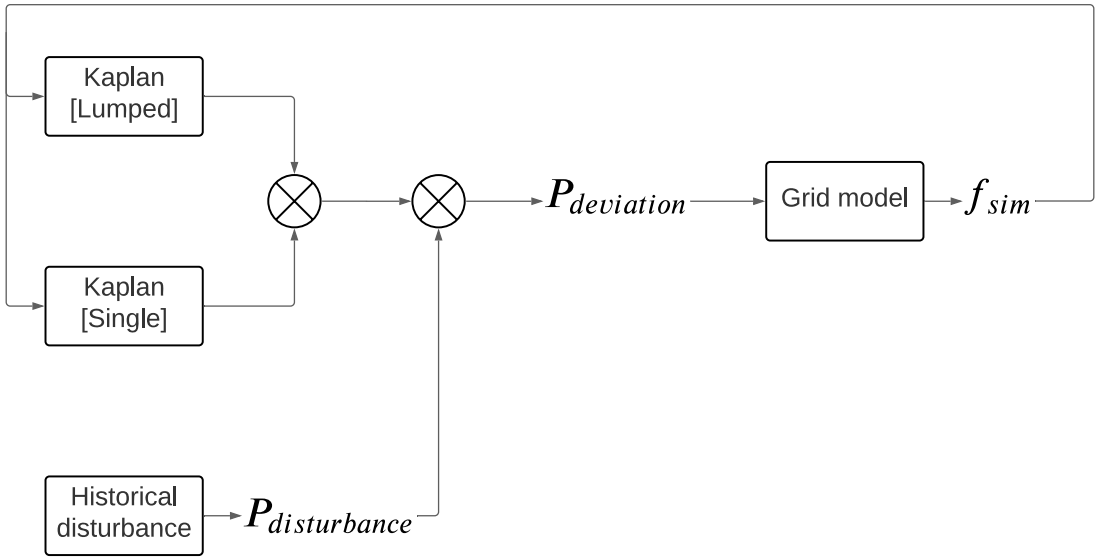

Figure 4.9: Model representing the case with only hydro-power

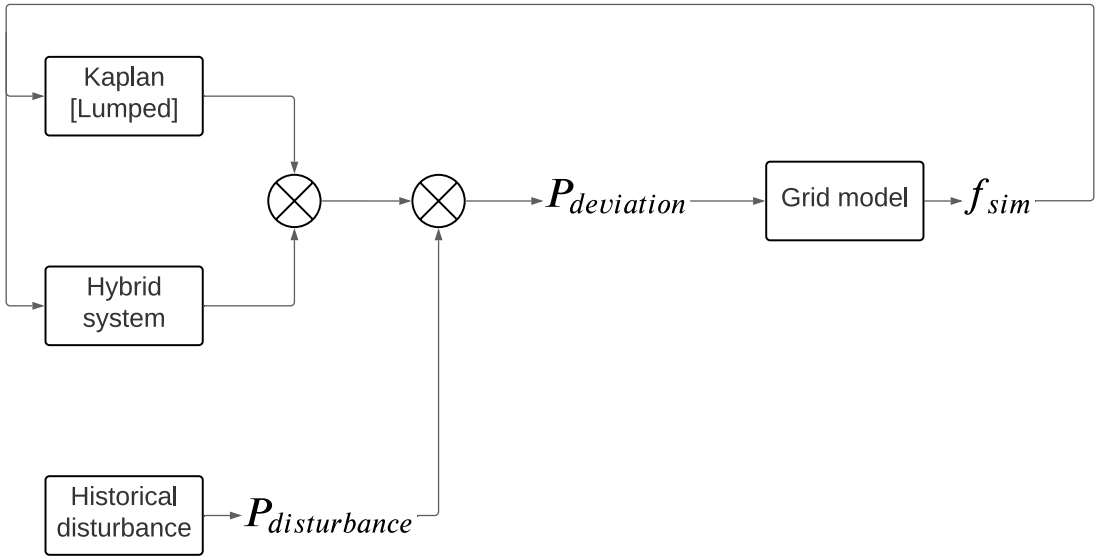

Figure 4.10: Model representing the case with hybrid system

Furthermore, as stipulated by SVK in the FCR-N test program the total system backlash and total FCR-N capacity needs to be calculated. This is done according to Equation (4.20), with the definitions of the variables used illustrated in Figure 4.11.

$$
\begin{aligned}
2D &= \frac{||\Delta P_1| - |\Delta P_2|| + ||\Delta P_3| - |\Delta P_4||}{2} \\
C_{\text{FCR-N}} &= \frac{|\Delta P_1| + |\Delta P_3| - 2D}{2}
\end{aligned}
\tag{4.20}
$$

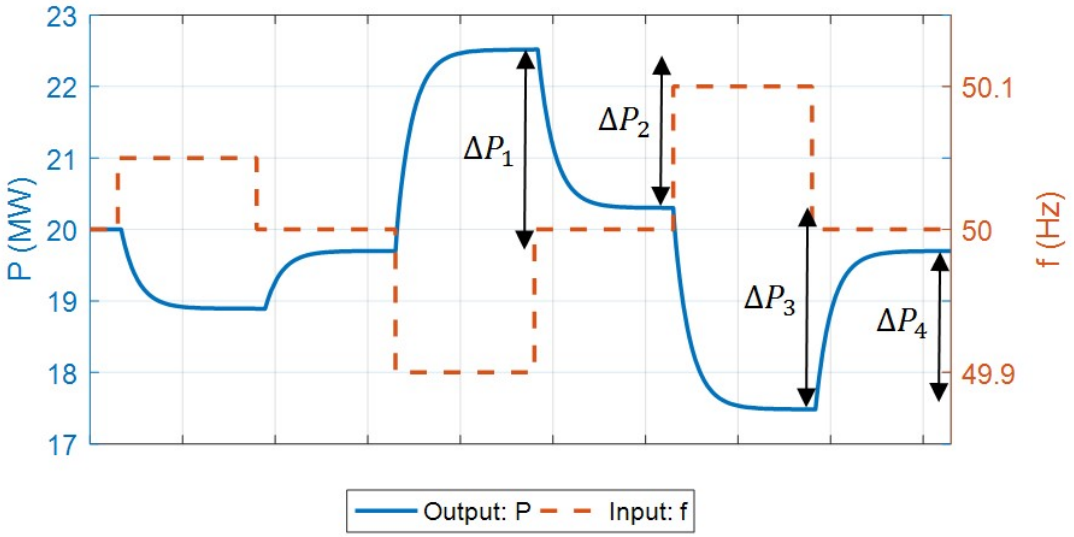

Figure 4.11: Variable definitions for pre-qualification test [65]

5 Simulation results

5.1 Model verification

By using the historical disturbance model as an input and comparing the measured frequency to the simulated, as seen in Figure 5.1, it is clear that the two are a good match. Therefore, the introduced historical disturbance model will yield a realistic operational scenario when used for the HBHS simulations. Furthermore, due to the accurate match between the two frequencies the model can be assumed to have passed its initial verification which means that any results gathered from the various tests are considered accurate enough for the purpose of the simulations, which is to give some indication regarding reduced maintenance of the hydro-power units.

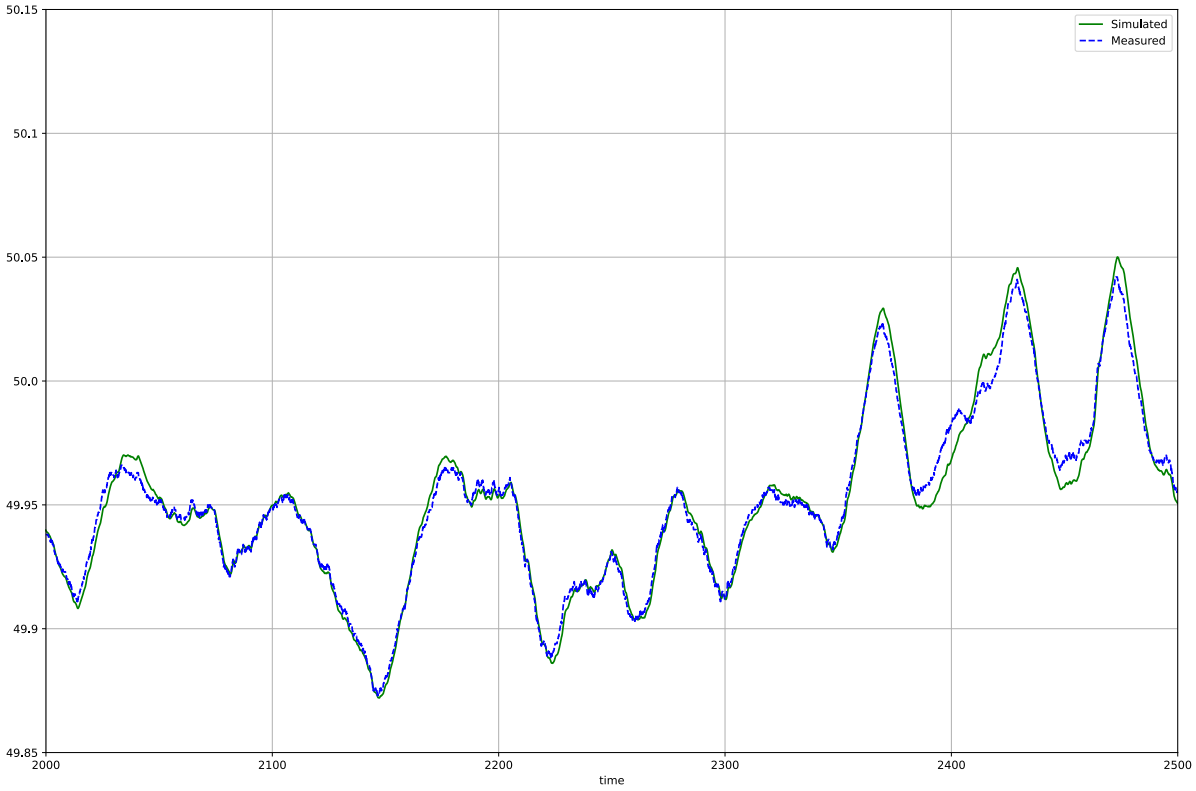

Figure 5.1: Frequency comparison between simulated and measured values

5.2 Model evaluation

5.2.1 Unit step

The first test for the two models involves a unit step with a value corresponding to the maximum frequency deviation, i.e., 0.1 Hz. The result, as illustrated in Figure 5.2, shows that the hybrid system performs better than the benchmark regarding the time dynamic. The slight steady state error exhibited by the system without the battery system is due to the included backlash system and while the hybrid system also yields a smaller, almost non-existing, error it should be noted that this is in-part due to the assumption of an ideal BESS with further research including the round-trip efficiency of the batteries.

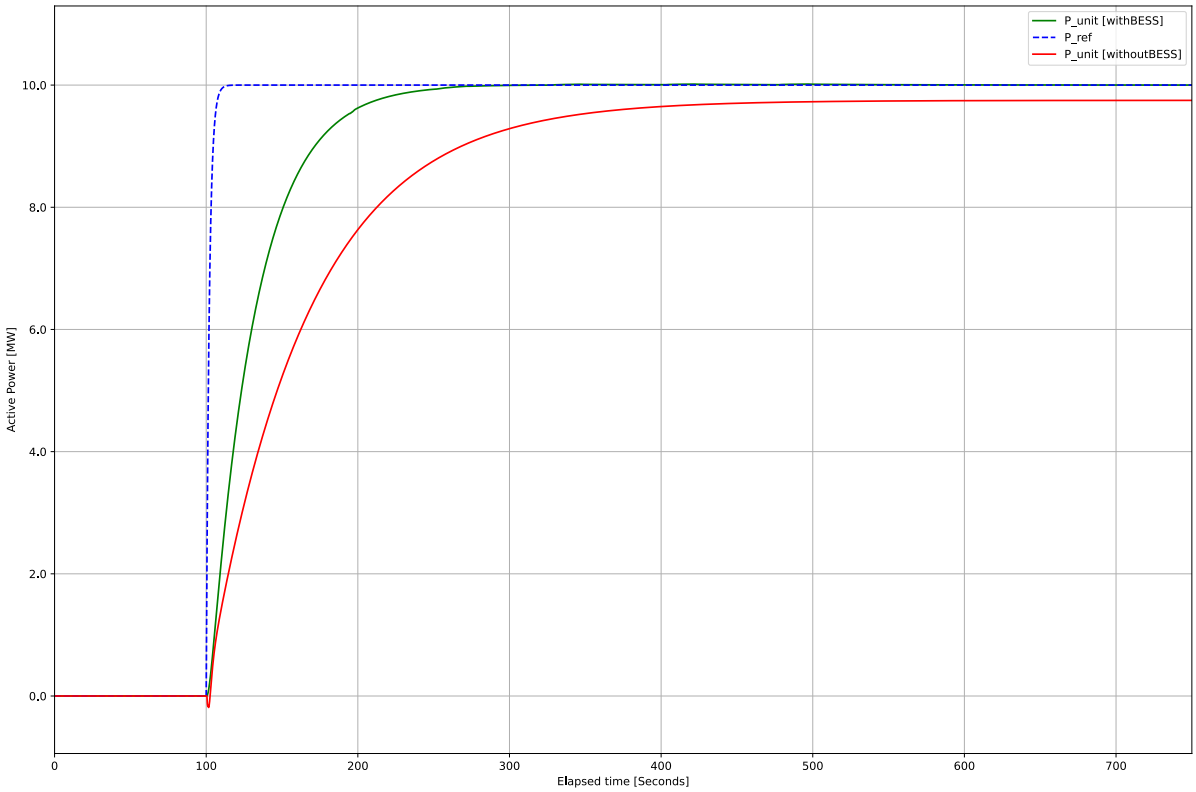

Figure 5.2: Unit step response for the two simulated systems

5.2.2 SVK benchmarking

The next test that is performed on the two systems is the pre-qualification test from SVK, in which a frequency sequence is fed to the systems to evaluate the performance as well as endurance. This sequence consists of steps of ±0.1 Hz, each with a duration of 60

minutes, as well as an initial step of 0.05 Hz which lasts for approximately 30 minutes. While the 0.1 **Hz** steps are required to have a duration of one hour, the remaining steps lasts until steady state has been achieved.

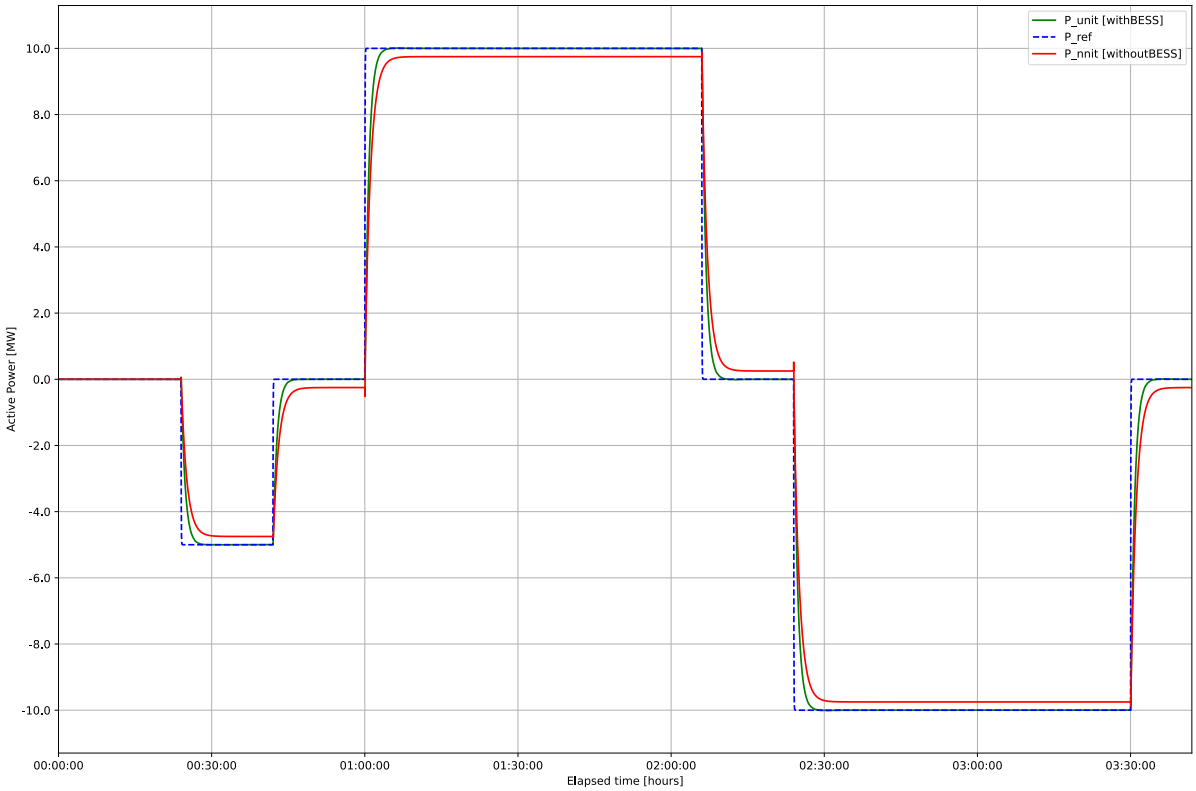

Figure 5.3: SVK frequency sequence response for the two simulated systems

As described in the SVK test program, based on the results of the tests the total backlash (2D) and the total FCR-N capacity are calculated according to the formulas found in Equation (4.20). The results, as displayed in Table 5.1, clearly shows that the amount of backlash for the hybrid system is less than for the hydro-only system.

Table 5.1: SVK benchmark key process indicators

Parameter	Without BESS	With BESS
2D	0.53 %	0 %
C_{FCR-N}	9.75 MW	10 MW

5.2.3 Historical simulation

Next up is simulating thirty days based on frequency measurements, taken from Fingrid for the month of August 2018, and comparing the two systems. The results, as shown in Figure 5.4 and Figure 5.5, show that both systems work similarly, although the hybrid systems have slightly higher peaks.

The slower regulation of the connected hydro-power units for the hybrid system is also evident, illustrated in the lower subplot, with each reference power step clearly visible. This is especially true for the Figure 5.5 in which the time period as been zoomed in, now showing the production during one hour.

Figure 5.4: Simulated frequency for August 2018 based on historical data - 5 hours

It is clear from the graphs that in the case of the hybrid system the BESS will do most of the regulation, with the hydro-power plant slowly ramping up/down the production when the deviation persists.

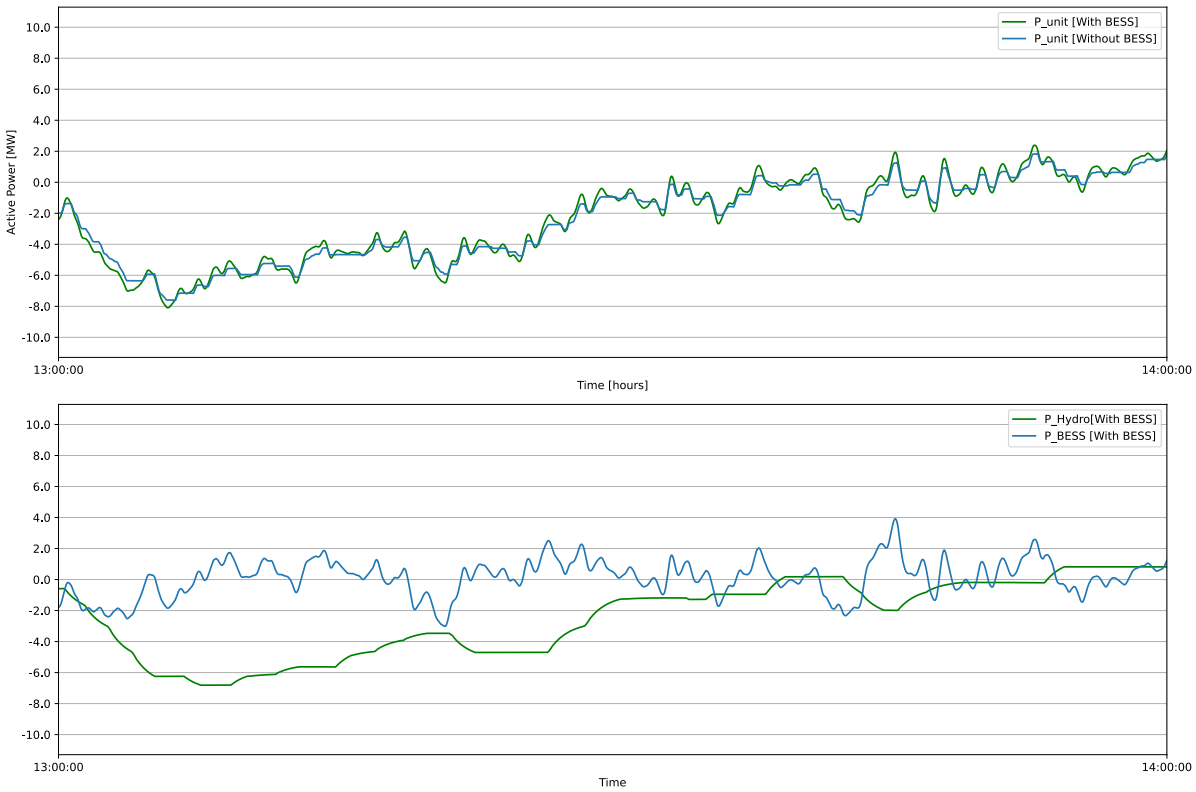

Figure 5.5: Simulated frequency for August 2018 based on historical data - 1 hour

5.2.4 Wear & tear calculations

During the month long simulation, data was collected regarding the vane movements and distance, as described in Section 4.6, for the two systems. A guide vane distance of 100% means that the vanes change from fully closed to fully open, so for example a distance of 1000% would mean that this is done ten times. This data, presented in Table 5.2, clearly shows a reduction in the distance travelled as well as the number of movements.

In total, the simulations show that the average distance moved per movement is 0.0639 % and 0.07 % for the guide- and runner-vanes respectively which is reasonable and consistent with earlier research [19][66].

5.3 Model comparison

In order to evaluate how good of a fit the simulations are to the installed units, the simulated values were overlaid with the measurements from the SVK benchmarking tests

Table 5.2: Wear & Tear key process indicators

Parameter	Without BESS	With BESS
Guide vane distance	5 595 %	957 %
Runner vane distance	5 501 %	956 %
Guide vane movements	84 567	5 411
Runner vane movements	75 981	5 321

from Lövön. The results are shown in Figure 5.6 and Figure 5.7 which illustrate the outputs from the hydro-power unit and the batteries and the combined system output respectively.

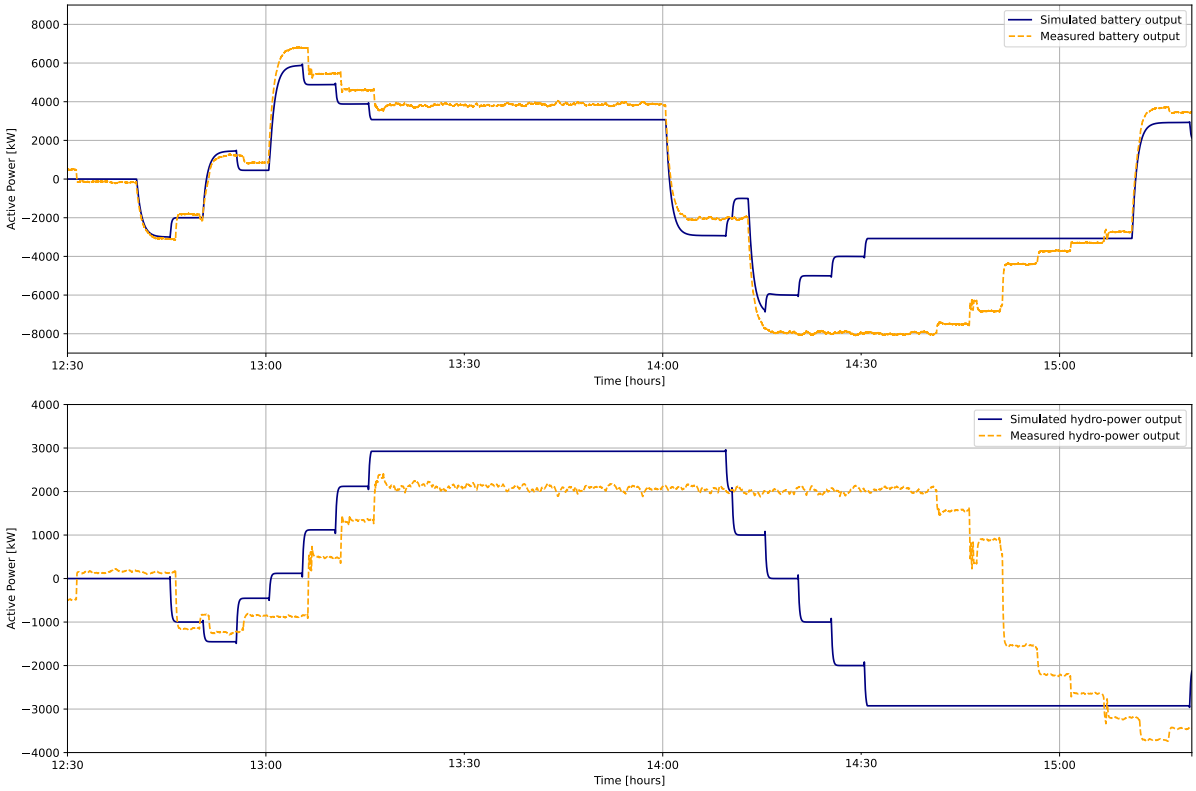

Figure 5.6: Comparison between installed and simulated hydro-power units and battery system

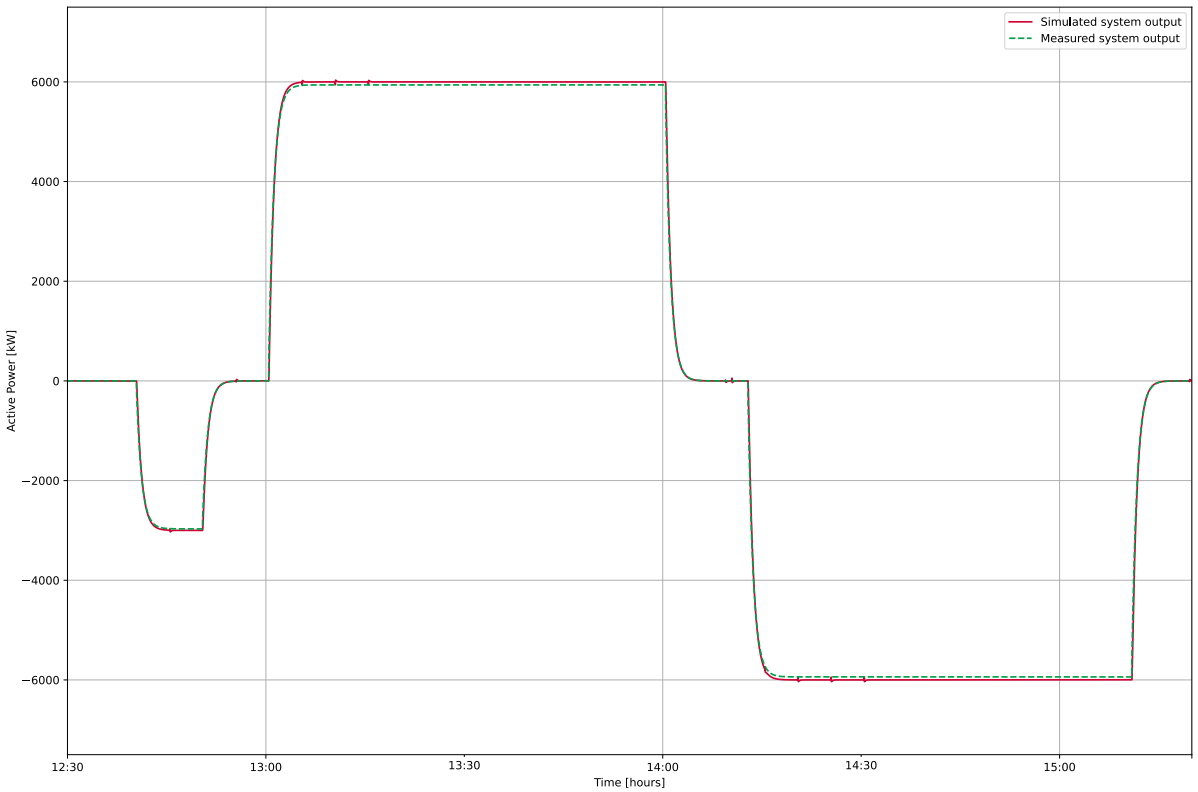

Figure 5.7: Comparison between installed hybrid-system output and simulated output

6 Project evaluation

The evaluation of the project at Lövön and Edsele can be split into two separate parts, where the first part contains information from interviews held with key personnel in the projects. The content of these interviews were then summarized in order to provide an overview with the lessons learned during the project and things to keep in mind for future projects that are similar. The second part of the evaluation will contain comments and remark on the measurements taken from Lövön during the testing as well as during a two-week period during which the unit was in commercial operations.

6.1 General comments and summary of interviews

Because the project started during the early parts of 2020, right as the virus disease COVID-19 became a pandemic, it experienced challenges that are not commonly found for projects in this type. The pandemic had a severe impact on deliveries of key materiel as well as introducing challenges regarding the physical work that needed to be done, as countries closed their borders. Overall, the involved parties handled these challenges admirably with delays kept at a minimum while still accomplishing the goals set out during planning.

During the early phase of the project the plan was for the installed units to only provide FCR-N, but based on the experience of the people involved the decision was made to also provide FCR-D and FFR. This turned out to be one of the best choices during the project as FCR-D is the only service that has currently been sold due to the increased price when compared to FCR-N. One of the key points to take from this project is to ensure a flexibility in the list of functions and services the units provide as the market is in constant change.

Furthermore, one thing that led to frustration was the lack of proper rules specific to the idea of delivering ancillary services from limited energy reservoirs, in this case - batteries. Because this is a relatively new concept, the requirements stipulated by the Swedish TSO are still based on the requirements that exists for normal units, such as hydro-power. This is exemplified by the pre-qualification tests required by the TSO in which the mechanical backlash of the batteries are tested, the results of which provide no usable information.

The projects at Lövön and Edsele were a pilot project, in which the type of hybrid structure described in this thesis were to be evaluated. The projects have been deemed a success within Uniper, not only due to the delivered functions and initial revenues being better than expected, but also because the projects were completed in such a short time in spite of the pandemic that made work considerably more difficult. The reason behind this success is in part attributed to the flexibility and information transparency between the various parties.

The willingness from the delivering party to work with and accommodate Uniper as the projects progressed has also been a large part in making the collaboration a success. During the early phase, a great deal of work was put into researching and making sure that the chosen company would be a good fit, and this paid off several times.

For future projects however, the recommendation is to allow for a longer planning phase and to ensure that each party is comfortable with the others. On the technical side, it is still too early to make any specific improvements as the units have only been in operation for a short time and thus not enough data has been gathered. One thing that is known however, is the need for a better collaboration between the hydro-power plants and the battery energy storage units. This could be better achieved by determining the optimal speed and precision that the turbines should exhibit, something that requires more data to properly determine.

Unlike the model developed and described in Chapter 4, the units installed at Lövön and Edsele aim to provide ancillary services beyond FCR-N, such as FFR, FCR-D Down and FCR-D Up. This means that the actual units are designed to meet the strict technical criteria set up by the Nordic TSOs. This meant that before being allowed to participate in the ancillary market, Uniper first needed to prove that the requirements for the various functions, as described in Section 2.2, were fulfilled. The results from these pre-qualification tests will be presented here, albeit not in full, with comments given regarding how well the units hold up to the technical requirements.

6.2 FCR-N

The first function that is tested and verified is the ability of the hybrid system to provide FCR-N. This is done in three different test configurations, each one with a specific set-point and configuration of active and inactive units.

While all the results from the tests are not presented in full here, the parts and results from the tests deemed the most important are highlighted and commented upon. The tests were performed at Lövön before the increase in installed power, meaning that the tests were done with an installed power of nine megawatts.

The first result, as illustrated in Figure 6.1, shows the first test in which the set-point is 3 MW with only the BESS active. While the hydro-power output remains zero at all times, due to it being inactive, the BESS follows the set-point admirably and provides all of the dispatched power which in this case is 3000 **kW**. Based on the technical requirements defined for FCR-N, the results presented here clearly shows that the battery storage performs as intended with 63 % reached after approximately 50 seconds which is well within the limit stipulated by SVK. This is illustrated more clearly in Figure 6.2 which provides a zoomed in view of the first set-point increase at 09:20.

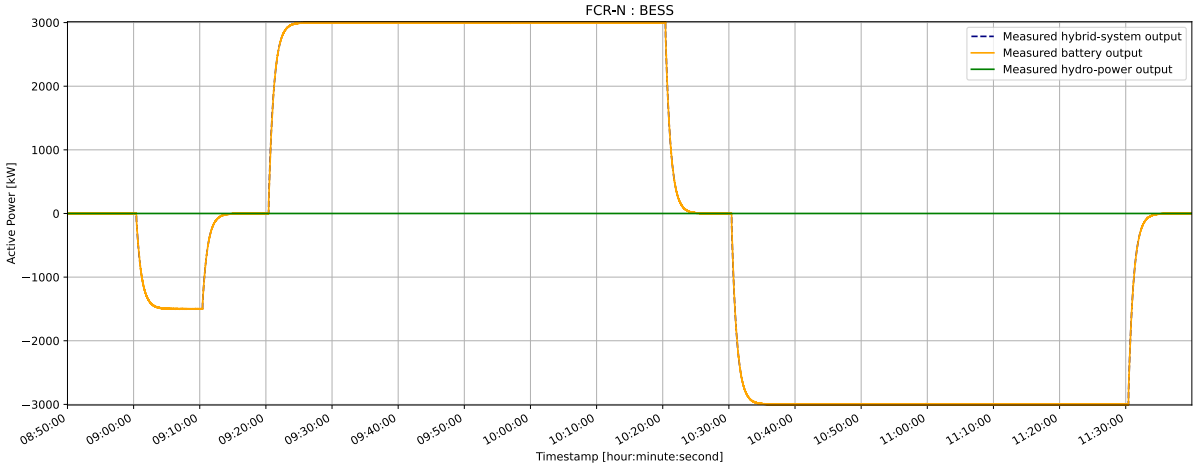

Figure 6.1: Test measurements for FCR-N with only BESS

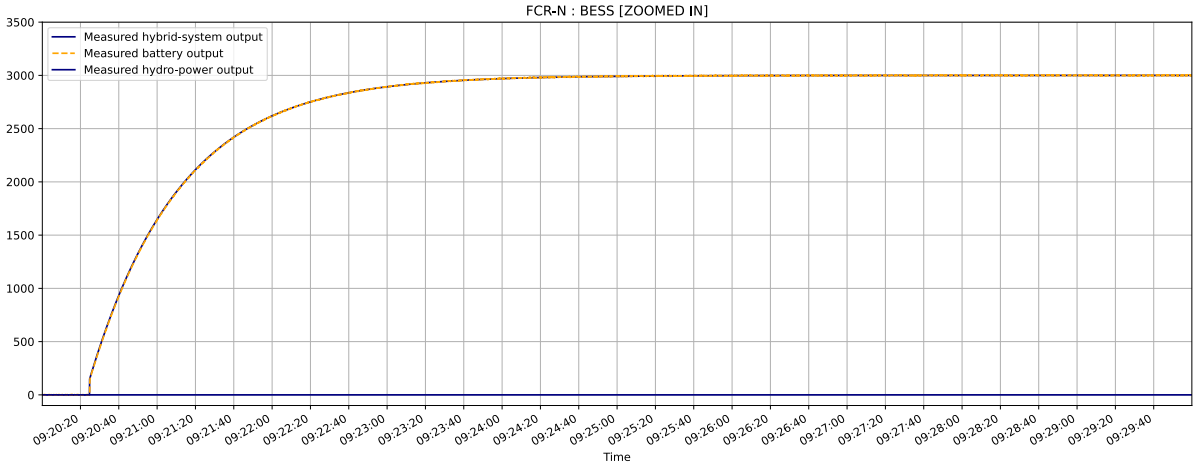

Figure 6.2: Test measurements for FCR-N with only BESS - Zoomed in

The next required test involves the battery system as well as one (out of two) enabled hydro-power unit and aims to validate the control of the interconnected hybrid system. The intended function is for the battery output to compensate for the production provided by the hydro-power unit, thereby making sure that the combined output for the hybrid system equals that which is required. This functionality is clearly illustrated in Figure 6.3, where the interconnected nature of the battery and hydro-power units is clearly illustrated. As the set-point changes, the battery system will adapt its output based on what the current output from the hydro-power unit is as can be seen clearly at 13:10.

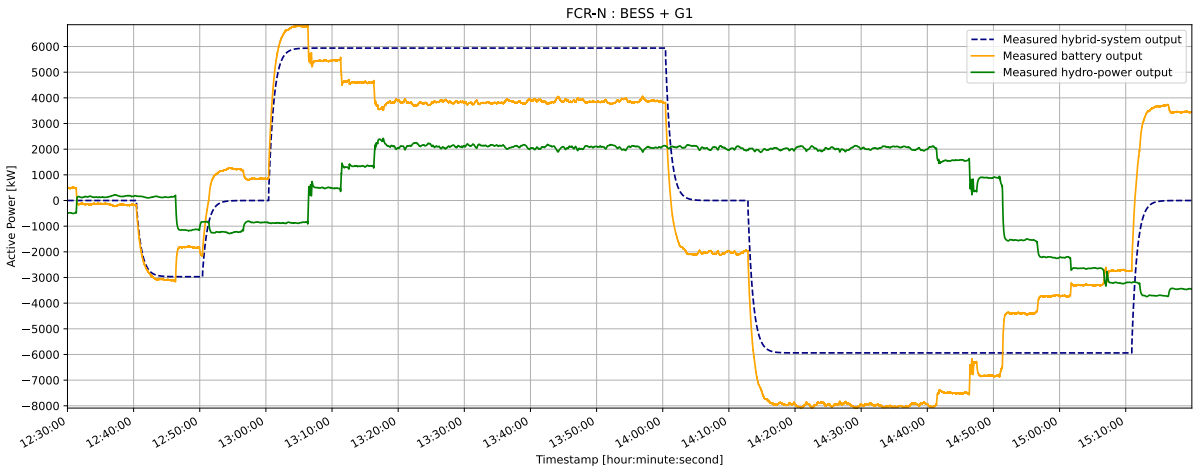

Figure 6.3: Test measurements for FCR-N with BESS and one hydro-power unit

6.3 FCR-D

The technical requirements for FCR-D, as stipulated by TSO and described in Section 2.2.2, require the units to be able to reach 50 % in under 5 seconds and 100 % in under 30 seconds. As is illustrated in Figure 6.4, this technical requirement (as well as the demand regarding endurance) is fulfilled by the installed system making it well suited for providing the FCR-D Down.

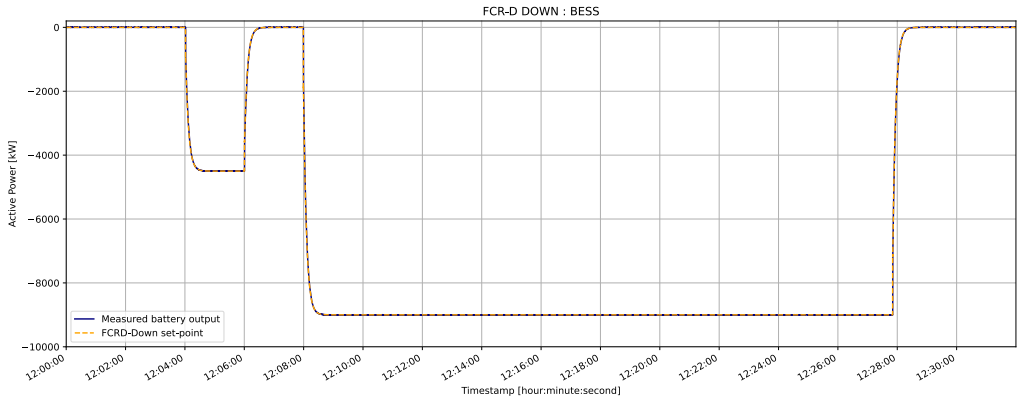

Figure 6.4: Test measurements for FCR-D Down with only BESS

6.4 FFR

The last function to be evaluated is the newly stipulated Fast Frequency Reserve or FFR. As described by SVK, there are three levels that this reserve operates on which are described in Section 2.2.5. These tests have different requirements whether the designed endurance is for 5 or 30 seconds, but as can be seen in Figure 6.5 and Figure 6.6 the units follow the set-point accurately and within the specified requirements.

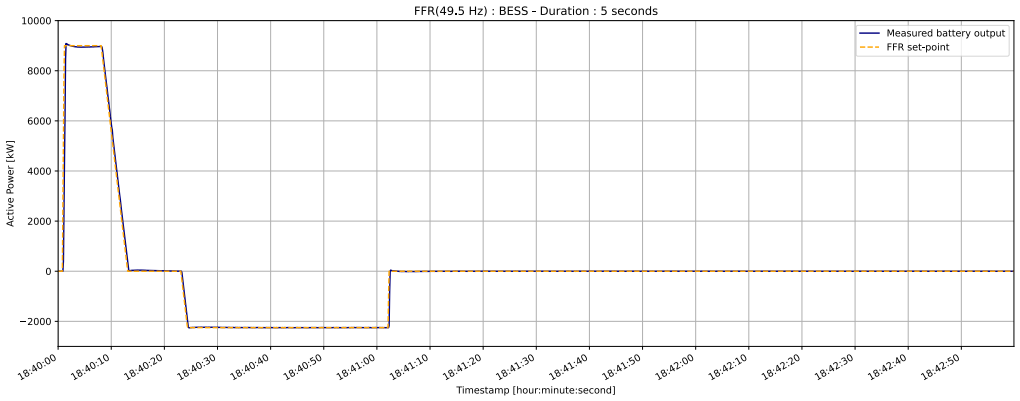

Figure 6.5: 5 second duration test of FFR

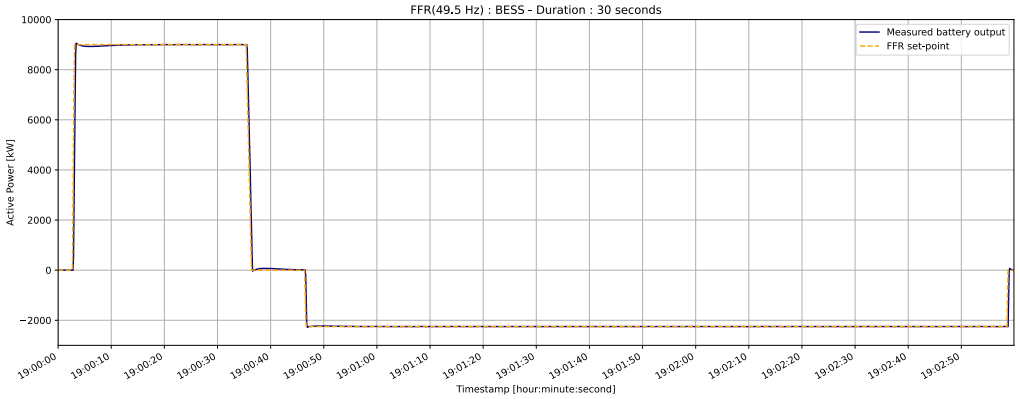

Figure 6.6: 30 second duration test of FFR

The tests, as described in the sections above, clearly show that the units deliver the functions they are designed for. This means that Uniper, with these units, can participate on all of the ancillary service markets currently active within the power grid.

7 Discussion

The purpose of this project was to evaluate and detail the project performed by Uniper, in which a battery energy storage system was installed in combination with a hydro-power plant with the goal of providing reserve power to the Nordic grid. This evaluation consisted of three parts; a technical study which aimed to detail and evaluate the components found in the hybrid system, an evaluation of the installed units as well as the development of a model for simulating the systems.

7.1 Technical study

While hydro-power can be considered to be a mature technology, the field of battery technologies is in constant flux with new and interesting technologies being researched and developed daily. As mentioned in Section 3.3, there are several interesting battery types in development, and as these mature they will most likely replace Li-ion as the battery of choice for stationary energy storage systems. In theory, the process of changing storage systems based on Li-ion should be fairly straight forward, which means that these kinds of hybrid systems offer easy upgrade capability allowing them to stay relevant as the technologies improve. Furthermore, as the grid moves towards more intermittent production the grid will need to adopt widespread use of energy storage systems, not only for the purpose of frequency regulation but also in order to ensure that no renewable production is lost.

7.2 Simulation

The models used throughout the simulations were based on existing models used throughout academia as well as newly developed models based on information received from the company which delivered the units and data gathered from measurements. The latter, which is mainly the power-plant controller, is not an exact copy of the real units due to the sparse nature of the information received. The power-plant controller used throughout the simulations is missing various functions (mainly the state-of-charge controller) for which the documentation and information were missing.

The hybrid system was compared to a traditional hydro-power only system throughout three different simulation scenarios; a unit-step, the bench-marking sequence provided by the Swedish TSO and then a month long simulation based on historical data. The unit-step simulation, illustrated in Section 5.2.1, shows a clear improvement for the hybrid system where not only the time-dynamics are improved but the steady state error is also reduced to zero. It should be noted however, that during the simulations the battery is assumed ideal which means that this zero steady state error might not be accurate. The steady state error found for the traditional system can be traced to the included backlash, see Section 4.2, which means that the model contains a non-linearity which complicates the system by introducing empty guide-vane movements, i.e., movements of the guide-vanes that do not change the produced power.

As with the simulation of a unit-step, described in Section 5.2.1, the backlash which is included in the turbine model is evident in the simulation of the TSO pre-qualification, as seen in Section 5.2.2. This simulation clearly shows, as with the unit-step, that the hybrid system performs better in terms of time-dynamics. The results of the TSO pre-qualification calculations regarding the total backlash and actual FCR-N capacity, detailed in Table 5.1, show that while the hydro-power fails to deliver the full amount, the hybrid system does. Although this is most likely not true in reality, as the batteries will never be ideal.

Furthermore, the simulation of August of 2018, as shown in Section 5.2.3, shows a good match between the two systems but with slightly higher peaks for the hybrid system. This is because the hybrid system contains two components, meaning that the output of the battery system is offset by the output from the connected hydro-power unit.

Overall, as seen in the figures depicting the various simulations, the model yields results in line with the expectation that the hybrid system should perform better than the traditional hydro-power only system.

Lastly, by comparing the outputs from the simulated models to the measured values taken from the pre-qualification tests performed at Lövön, as illustrated in Section 5.3, the model is evaluated based on how good the model represents the actual units. The results show, clearly, that the model is not an exact copy of the installed units but that it shows the same characteristics that the installed units show. This is illustrated mainly in Figure 5.6 which compares the battery and hydro-power outputs of the simulations and the physical systems. The main source of the difference between the two cases is most likely the missing state-of-charge controller, but also the fact that the implemented controller is based on sparse information due to confidentiality concerns. However, regardless of the difference between simulation and measurements, this model is still considered verifiable enough that conclusions can be drawn from the results.

Further research should aim to develop a complete model for the power-plant controller, where the state-of-charge controller should be the main focus. This is because the state-of-

charge controller is one of the most important parts of any battery energy storage system as this controller will have a large impact on the health of the batteries and therefore the length of time during which the batteries are usable. Ensuring an optimal operation of this controller is therefore of vital importance for the entire energy storage system and therefore also the hybrid system.

7.3 Evaluation

By talking to two of the main people involved in the two projects at Lövön and Edsele and summarizing the interviews, the project was evaluated on a project management basis but also provided information that helped to evaluate the technical functions. Even with the ongoing pandemic, the projects went without any larger problems and are considered a great success both internally and externally. The most important point that should be considered for any future projects of this type is the need for flexibility of the delivered functions. The initial plan was to only provide FCR-N, something that was changed early in the project which turned out to be a very important change as the current delivered service is FCR-D. By installing units that have a great flexibility of the delivered functions, Uniper has made sure that they can be active on whichever service market that pays best, which ensures optimal profitability.

The importance of the contractor chosen for delivering the units is also a important point, and as can be seen in this project: cheapest is not always best. Any company attempting a similar project should therefore ensure that adequate time and resources are spent in order to find the external partner that shows the most willingness to work together towards a common goal.

The measurements presented in Chapter 6 show that the installed units clearly fulfill the technical requirements for each of the functions which the units aim to provide.

8 Conclusion

The existing research and information regarding the various components that make up the hybrid system, such as the batteries and hydro-power units, was collated and summarized in the technical study. This study was mainly focused on the technical aspect, but with the sustainability and versatility aspects also being discussed.

This information, as well as additional information regarding the modelling of hydro-power units participating in the FCR-N market, was used as a foundation for the model developed, that aimed to describe the hybrid system which was installed at Lövön. This model proved a good match to previous models as well as the actual units, and was verified using measurements of the grid frequency as well as measurements from the pre-qualification tests. Overall, the models show a large decrease (close to 80 % for the vane distance and 90 % for the number of movements) for the maintenance key process indicators.

The developed power plant controller that was used throughout the simulations is based on the actual units, but is not an exact copy, due mainly to confidentiality reasons as well as lacking information. Instead, the model is based on some information from the manufacturer but also general control schemes and practices. While the model provides realistic results that share characteristics with the actual units, several improvements must be made in order to yield a digital twin of the installed units.

This Thesis has clearly shown that this type of hybrid system has many of advantages as the batteries and hydro-power complement each other in such a way as to provide a synergy that is highly beneficial the the power-grid.

The project performed by Uniper in collaboration with their contractors has been successful in terms of technical requirement fulfillment and the project being completed in short time. Furthermore, this project has clearly shown several benefits that this type of system provides; such as increased grid stability resulting from the rapid response time and high performance of the ancillary services as well as a reduction of wear and tear for the hydropower turbines.

8.1 Further Research

Because the developed model, specifically the power-plant controller, does not contain all the same functions as (nor behaves like) the installed units, this should provide a great starting point for future research. The biggest function currently missing - and which should be the next step in the development of this model - is the missing state-of-charge controller.

Furthermore, having a model which is a complete (or as close as one can get) implementation of the actual units will provide a good test-bed for future research into how the control scheme for this type of hybrid system should be implemented in order to provide the biggest improvements.

Bibliography

[1] S. Kraftnät. (2019). 'Storfinnforsen – midskog.' English, [Online]. Available: https://www.svk.se/en/grid-development/grid-projects/storfinnforsen--midskog/ (visited on 17/01/2021).

[2] Statnett. (2018). 'How the power system works.' English, [Online]. Available: https://www.statnett.no/en/about-statnett/get-to-know-statnett-better/how-the-power-system-works/ (visited on 17/01/2020).

[3] E. F. Norway. (2019). 'The electricity grid.' English, [Online]. Available: https://energifaktanorge.no/en/norsk-energiforsyning/kraftnett/ (visited on 17/01/2020).

[4] R. S. A. of Engineering Sciences, 'Sweden's future electrical grid: A project report,' English, 2017. [Online]. Available: https://www.iva.se/en/published/swedens-future-electrical-grid--a-project-report/ (visited on 18/01/2021).

[5] SVK, *Map of the national grid*, http://www.svk.se/om-kraftsystemet/om-transmissionsnatet/transmissionsnatskarta/, 2020. (visited on 29/12/2020).

[6] S. E. M. Inspectorate, 'Utvärdering av effekterna av elområdesindelningen,' Swedish, 2014. [Online]. Available: http://www.ei.se/sv/Publikationer/Rapporter-och-PM/rapporter-2014/utvardering-av-effekterna-av-elomradesindelningen-ei-r2014-08/ (visited on 18/01/2021).

[7] Hou710, 2015. [Online]. Available: https://commons.wikimedia.org/wiki/File:Hou710_ElectricityPriceArea.svg (visited on 18/01/2021).

[8] I. Newton, *The Mathematical Principles of Natural Philosophy*, N. W. Chittenden, Ed. New York: Daniel Adee, 1846.

[9] ENTSO-E, 'Fast frequency reserve – solution to the nordic inertia challenge,' English, 2019.

[10] S. Kraftnät, *Agreement on balance responsibility for electricity*, Swedish, PDF. [Online]. Available: https://www.svk.se/aktorsportalen/elmarknad/balansansvar/balansansvarsavtal/ (visited on 28/12/2020).

[11] Energimyndigheten, S. kraftnät and H. och vattenmyndigheten, 'Vattenkraftens reglerbidrag och värde för elsystemet,' Swedish, 2019. [Online]. Available: https://energimyndigheten.a-w2m.se/FolderContents.mvc/Download?ResourceId=104670 (visited on 20/01/2021).

[12] S. Kraftnät, *Overview of the requirements on reserves.* English, PDF, 2018. [Online]. Available: https://www.svk.se/siteassets/4.aktorsportalen/systemdrift-o-elmarknad/information-om-stodtjanster/reserve-markets.pdf (visited on 21/01/2021).

[13] A. M. Ersdal, L. Imsland, K. Uhlen, D. Fabozzi and N. F. Thornhill, 'Model predictive load-frequency control taking into account imbalance uncertainty.,' *Control Engineering Practice*, 2016.

[14] ENTSO-E, 'Technical requirements for fast frequency reserve provision in the nordic synchronous area,' English, 2019. [Online]. Available: https://www.svk.se/siteassets/aktorsportalen/tekniska-riktlinjer/ovriga-instruktioner/technical-requirements-for-fast-frequency-reserve-provision-in-the-nordic-synchronous-area-1.pdf (visited on 18/01/2021).

[15] European commision, *Commission regulation (eu) 2017/1485 of 2 august 2017 establishing a guideline on electricity transmission system operation*, https://eur-lex.europa.eu/legal-content/EN/TXT/?uri=CELEX:32017R1485, 2017. (visited on 09/01/2021).

[16] S. Kraftnät, *Information om stödtjänster från energilager*, Swedish, PDF, 2020. [Online]. Available: http://www.svk.se/siteassets/aktorsportalen/elmarknad/information-om-stodtjanster/information--om-stodtjanster-fran-energilager.pdf (visited on 22/01/2021).

[17] I. E. Association, 'Renewables 2020, Analysis and forecast to 2025,' Tech. Rep., 2020.

[18] ENTSO-E, 'Technical requirements for frequency containment reserve provision in the nordic synchronous area,' English, 2021. [Online]. Available: https://www.svk.se/siteassets/aktorsportalen/elmarknad/information-om-stodtjanster/forkvalificering/fcr-technical-requirements_draft_2021.pdf (visited on 05/03/2021).

[19] D. Laban, 'Hydro/battery hybrid systems for frequency regulation,' M.S. thesis, UPC, Escola Tècnica Superior d'Enginyeria Industrial de Barcelona, Departament d'Enginyeria Elèctrica, 2019. [Online]. Available: http://hdl.handle.net/2117/167410 (visited on 07/02/2021).

[20] Fortum. (). 'Batterilösningen i forshuvud stärker kapaciteten för nordisk vattenkraft.' Swedish, [Online]. Available: https://www.fortum.se/om-oss/hallbarhet/investeringar-i-vattenkraft/var-unika-batterilosning-vid-forshuvuds-kraftverk (visited on 04/03/2021).

[21] C. Nunez. (2020). 'Hydropower, explained,' [Online]. Available: https://www.nationalgeographic.com/environment/global-warming/hydropower/ (visited on 10/09/2020).

[22] S. E. Agency, 'Energy in sweden 2020 - an overview,' English, 2020. [Online]. Available: https://energimyndigheten.a-w2m.se/FolderContents.mvc/Download?ResourceId=174155.

[23] IEA, *Data and statistics*, https://www.iea.org/data-and-statistics, 2020. (visited on 29/12/2020).

[24] M. O. Tomi Mäkinen Aki Leinonen, 'International conference on environment and electrical engineering (eeeic),' in *Modelling and benefits of combined operation of hydropower unit and battery energy storage system on grid primary frequency control*, 2020.

[25] U. D. of Energy. (2020). 'Types of hydropower plants,' [Online]. Available: https://www.energy.gov/eere/water/types-hydropower-plants (visited on 06/01/2021).

[26] X. Niu, 'Key Technologies of the Hydraulic Structures of the Three Gorges Project,' en, *Engineering*, vol. 2, no. 3, pp. 340–349, Sep. 2016, ISSN: 2095-8099. DOI: 10.1016/J.ENG.2016.03.006. [Online]. Available: http://www.sciencedirect.com/science/article/pii/S2095809916311687 (visited on 02/02/2021).

[27] Mariordo, 2017. [Online]. Available: https://commons.wikimedia.org/wiki/File:2017_Aerial_view_Hoover_Dam_4774.jpg (visited on 02/02/2021).

[28] A. Kjølle, *Hydropower in Norway: Mechanical equipment*. Trondheim, Trøndelag, 2001.

[29] Jahobr, 2016. [Online]. Available: https://commons.wikimedia.org/wiki/File:PeltonSketch.svg (visited on 29/03/2021).

[30] ——, 2019. [Online]. Available: https://commons.wikimedia.org/wiki/File:Propeller_Turbine_2.svg (visited on 02/02/2021).

[31] D. N. K. P Sridharan, 'Mitigation of vibration on bulb turbine in small hydro electric power plants,' *International Journal of Engineering and Technology (IJET)*, 2013.

[32] 'Electric machinery fundamentals,' in. McGrawHill, 2012, ch. 4.

[33] G. Mottershead, S. Bomben, I. Kerszenbaum and G. Klempner, 'Generator design and construction,' in *Handbook of large hydro generators - Operation and Maintenance*. 2020.

[34] *IEC/IEEE Guide for Computer-based Control for Hydroelectric Power Plant Automation*, eng, 2013. DOI: 10.1109/IEEESTD.2013.6617651.

[35] 'Hydropower status report - sector trends and insights,' International Hydropower Association, Tech. Rep., 2018.

[36] C. Naschert, 'With ambitions offshore, floating solar makes its first splashes in europe,' *S&P Global*, 5th Oct. 2020. [Online]. Available: https://www.spglobal.com/marketintelligence/en/news-insights/latest-news-headlines/with-ambitions-offshore-floating-solar-makes-its-first-splashes-in-europe-59512639 (visited on 05/03/2020).

[37] *Hyosung Heavy Industries*, en. [Online]. Available: http://www.hyosungheavyindustries.com (visited on 16/03/2021).

[38] X. Luo, J. Wang, M. Dooner and J. Clarke, 'Overview of current development in electrical energy storage technologies and the application potential in power system operation,' *Applied Energy*, vol. 137, pp. 511–536, Jan. 2015. DOI: 10.1016/j.apenergy.2014.09.081.

[39] L. Beltramin, 'State-of-the-art of the flywheel/li-ion battery hybrid storage system for stationary applications,' 2018.

[40] X. Luo, J. Wang, M. Dooner and J. Clarke, 'Overview of current development in electrical energy storage technologies and the application potential in power system operation,' *Applied Energy*, vol. 137, pp. 511–536, 2015, ISSN: 0306-2619. DOI: 10.1016/j.apenergy.2014.09.081. [Online]. Available: http://www.sciencedirect.com/science/article/pii/S0306261914010290.

[41] Infineon. (28th Jan. 2021). 'Battery management system (bms),' [Online]. Available: https://www.infineon.com/cms/en/applications/solutions/battery-management-system/ (visited on 28/01/2021).

[42] U.S Department of Energy, U.S Department of Energy. [Online]. Available: https://www.sandia.gov/ess-ssl/global-energy-storage-database-home/ (visited on 27/01/2021).

[43] G. J. May, A. Davidson and B. Monahov, 'Lead batteries for utility energy storage: A review,' en, *Journal of Energy Storage*, vol. 15, pp. 145–157, Feb. 2018, ISSN: 2352-152X. DOI: 10.1016/j.est.2017.11.008. [Online]. Available: http://www.sciencedirect.com/science/article/pii/S2352152X17304437 (visited on 01/02/2021).

[44] R. Younesi, G. M. Veith, P. Johansson, K. Edström and T. Vegge, 'Lithium salts for advanced lithium batteries: Li–metal, Li–O2, and Li–S,' en, *Energy & Environmental Science*, vol. 8, no. 7, pp. 1905–1922, Jul. 2015, ISSN: 1754-5706. DOI: 10.1039/C5EE01215E.

[45] M. Wakihara, 'Recent developments in lithium ion batteries,' *Materials Science and Engineering: R: Reports*, vol. 33, no. 4, pp. 109–134, 2001, ISSN: 0927-796X. DOI: 10.1016/S0927-796X(01)00030-4. [Online]. Available: http://www.sciencedirect.com/science/article/pii/S0927796X01000304.

[46] P. Roy and S. K. Srivastava, 'Nanostructured anode materials for lithium ion batteries,' en, *Journal of Materials Chemistry A*, vol. 3, no. 6, pp. 2454–2484, Jan. 2015, ISSN: 2050-7496. DOI: 10.1039/C4TA04980B.

[47] *What is a flow battery? – The International Flow Battery Forum*, en-GB. [Online]. Available: https://flowbatteryforum.com/what-is-a-flow-battery/ (visited on 01/02/2021).

[48] U. D. o. E. Jefferson Lab. (2021). 'Hydrogen.' English, [Online]. Available: https://pubchem.ncbi.nlm.nih.gov/element/Hydrogen#section=History (visited on 12/04/2021).

[49] Hybrit. (2021). 'Research project 1.' English, [Online]. Available: https://www.hybritdevelopment.se/en/research-project-1/ (visited on 12/04/2021).

[50] K. Sugarman. (2016). 'Hydrogen through electrolysis.' English, [Online]. Available: https://www.oceangeothermal.org/hydrogen-energy-electrolysis/ (visited on 12/04/2021).

[51] P. Breeze, 'Chapter 8 - hydrogen energy storage,' in *Power System Energy Storage Technologies*, P. Breeze, Ed., Academic Press, 2018, pp. 69–77, ISBN: 978-0-12-812902-9. DOI: https://doi.org/10.1016/B978-0-12-812902-9.00008-0.

[52] FCHEA. (2019). 'Fuel cell & hydrogen energy basics.' English, [Online]. Available: https://www.fchea.org/h2-day-2019-events-activities/2019/8/1/fuel-cell-amp-hydrogen-energy-basics (visited on 12/04/2021).

[53] M. Farhadi and O. Mohammed, 'Energy Storage Technologies for High Power Applications,' *IEEE Transactions on Industry Applications*, vol. 52, pp. 1–1, Jan. 2015. DOI: 10.1109/TIA.2015.2511096.

[54] A. Reindl, H. Meier and M. Niemetz, 'Scalable, Decentralized Battery Management System Based on Self-organizing Nodes,' en, in *Architecture of Computing Systems – ARCS 2020*, A. Brinkmann, W. Karl, S. Lankes, S. Tomforde, T. Pionteck and C. Trinitis, Eds., ser. Lecture Notes in Computer Science, Cham: Springer International Publishing, 2020, pp. 171–184, ISBN: 9783030527945. DOI: 10.1007/978-3-030-52794-5_13.

[55] E. Chatzinikolaou and D. J. Rogers, 'A Comparison of Grid-Connected Battery Energy Storage System Designs,' *IEEE Transactions on Power Electronics*, vol. 32, no. 9, pp. 6913–6923, Sep. 2017, ISSN: 1941-0107. DOI: 10.1109/TPEL.2016.2629020.

[56] L. S. Xavier, W. C. S. Amorim, A. F. Cupertino, V. F. Mendes, W. C. do Boaventura and H. A. Pereira, 'Power converters for battery energy storage systems connected to medium voltage systems: A comprehensive review,' *BMC Energy*, vol. 1, no. 1, p. 7, Jul. 2019, ISSN: 2524-4469. DOI: 10.1186/s42500-019-0006-5.

[57] S. Ali and K. Vijayarajan, *Bipolar multicarrier PWM techniques for cascaded quasi-Z-source multilevel inverter*. Mar. 2013, p. 240, ISBN: 9781467349215. DOI: 10.1109/ICCPCT.2013.6528977.

[58] H. Abu Bakar Siddique, A. R. Lakshminarasimhan, C. I. Odeh and R. W. De Doncker, 'Comparison of modular multilevel and neutral-point-clamped converters for medium-voltage grid-connected applications,' in *2016 IEEE International Conference on Renewable Energy Research and Applications (ICRERA)*, 2016, pp. 297–304. DOI: 10.1109/ICRERA.2016.7884555.

[59] H. E. Melin, 'State-of-the-art in reuse and recycling of lithium-ion batteries – a research review,' English, Circular Energy Storage, research rep., Jun. 2019. [Online]. Available: http://www.energimyndigheten.se/globalassets/forskning--innovation/overgripande/state-of-the-art-in-reuse-and-recycling-of-lithium-ion-batteries-2019.pdf.

[60] BloombergNEF. (2019). 'A behind the scenes take on lithium-ion battery prices.' English, [Online]. Available: https://about.bnef.com/blog/behind-scenes-take-lithium-ion-battery-prices/ (visited on 05/02/2020).

[61] L. Saarinen, P. Norrlund and U. Lundin, 'Allocation of Frequency Control Reserves and its Impact on Wear on a Hydropower Fleet,' *IEEE Transactions on Power Systems*, vol. PP, pp. 1–1, May 2017. DOI: 10.1109/TPWRS.2017.2702280.

[62] L. Saarinen, P. Norrlund, U. Lundin, E. Agneholm and A. Westberg, 'Full-scale test and modelling of the frequency control dynamics of the Nordic power system,' in *2016 IEEE Power and Energy Society General Meeting (PESGM)*, ISSN: 1944-9933, Jul. 2016, pp. 1–5. DOI: 10.1109/PESGM.2016.7741711.

[63] M. Syed, E. Guillo-Sansano, G. Burt, Y. Wang and Y. Xu, *Analysis of Responsibilization within Primary Frequency Control*. Oct. 2018, p. 6. DOI: 10.1109/ACEPT.2018.8610672.

[64] L. Saarinen, P. Norrlund and U. Lundin, 'Field measurements and system identification of three frequency controlling hydropower plants,' *IEEE Transactions on Energy Conversion*, vol. 30, no. 3, pp. 1061–1068, 2015. DOI: 10.1109/TEC.2015.2425915.

[65] SVK. (2020). 'Test program for provision of fcr-n.' English, [Online]. Available: https://www.svk.se/siteassets/aktorsportalen/systemdrift-o-elmarknad/information-om-stodtjanster/forkvalificering/test-program-for-provision-of-fcr-n.docx (visited on 22/03/2021).

[66] W. Yang, P. Norrlund, L. Saarinen, J. Yang, W. Guo and W. Zeng, 'Wear and tear on hydro power turbines – Influence from primary frequency control,' en, *Renewable Energy*, vol. 87, pp. 88–95, Mar. 2016, ISSN: 0960-1481. DOI: 10.1016/j.renene.2015.10.009.

Appendix A

Task description

University of South-Eastern Norway

Faculty of Technology, Natural Sciences and Maritime Sciences, Campus Porsgrunn

FMH606 Master's Thesis

Title: Evaluation of battery storage in combination with hydro-power systems.

USN supervisor: Dietmar Winkler

External partner: Norconsult, Uniper

Task background:
Uniper is an energy company based in Germany, but who operates a range of assets in Sweden. These assets include stakes in Nuclear power stations but also more importantly hydro-power systems. Uniper has been working on three projects where battery banks are combined with hydro-power systems. The idea is that by doing this Uniper will be able to sell frequency regulation from machines that are not designed for fast regulation. By charging the batteries they can deliver fast frequency changes while the hydro-power turbines guide-vanes can regulate slowly, limiting wear on the machines. This Master's Thesis aims to describe and evaluate the usage of batteries in combination with hydropower.

Task description:
The Master's Thesis should aim to contain the following parts:

- A technical study about how to combine hydropower and batteries. This should include technical descriptions of the various components.
- Description of the future scenario for battery storage presenting the economical and technological improvements one can expect.
- Description of the technology from a sustainability perspective, detailing the pros and cons as well as determining if the batteries can be used with solar power.
- Determination of the gains of the technology and whether the batteries can be used for things other than frequency regulation, like reserve power or control of the intake gates.
- Explanations regarding the importance of placing the batteries close to the hydro-power system.
- Evaluation of Uniper's project, determining what could have been done better and what lessons was learnt.
- Verify developed model using measurements from Unipers facilities.
- Development of a model over the implemented system for use in comparison to the measured values.

Student category: EPE (reserved for Lars Jonatan Hellborg)

The task is suitable for online students (not present at the campus):
Yes (is to be done in Sweden)

Practical arrangements:
The thesis is to be written in Östersund, Sweden.

Supervision:
As a general rule, the student is entitled to 15-20 hours of supervision. This includes necessary time for the supervisor to prepare for supervision meetings (reading material to be discussed, etc).

Signatures:
Supervisor (date and signature):
2021-01-28

Student (write clearly in all capitalized letters):
LARS JONATAN HELLBORG

Student (date and signature):
2021-01-28 Jonatan Hellborg